Final Report submitted to

EMPRIMUS LLC

Simulation of Transformer GIC Mitigation Using Neutral DC Current and Voltage Harmonic Level to Switch in a Capacitor to the Grounding Circuit

Final Report

Prepared by
Athula D. Rajapakse and Nuwan Perera
190 Craigmohr Dr., Winnipeg, MB, CANADA R3T 6C1

08 Aug, 2011

Third Party Disclaimer:
The content of this document is not intended for the use of, nor is it intended to be relied upon by any person, firm or corporation, other than the authors of the report and EMPRIMUS LLC.

Authors of this report deny any liability whatsoever to any parties for damages or injury suffered by such third party arising from the use of this document by the third party.

Confidentiality:
This document is restricted to the confidential use of the authors and EMPRIMUS LLC. Any retention, reproduction, distribution or disclosure to third parties is prohibited without written authorization of EMPRIMUS LLC.

1. Introduction

During a geomagnetic storm, a portion of the earth could experience a time varying magnetic field, inducing electric fields that sometime exceeds 6 V/km on the earth surface [1, 2]. This earth surface potential (ESP) acts as a voltage source applied between neutrals of the Y-connected transformer windings that may be located at opposite ends of a long transmission line. The resulting current that flows between the neutrals is called a geomagnetically induced current (GIC), which has a very low frequency (few milli-Hz) variation. Thus, GICs appear as quasi-DC in comparison the power frequency. GIC magnitudes over 100 A per phase have been measured in some three phase power systems [1, 2]. When this quasi-DC current enters a transformer, it may shift the operating point of the magnetic characteristics to one side, if the zero sequence reluctance of the transformer is low. This may ultimately cause the transformer to enter the half cycle saturation region. The resulting large asymmetrical exciting current increases the reactive power consumption and generates significant levels of harmonics and hot spot heating [1-5]. In addition to transformers, other equipment such as static VAR compensators and capacitor banks are susceptible to false tripping due to increased harmonic levels during geomagnetic disturbances [1,2]. One example of power disruption due to GIC is the collapse of Hydro Quebec power system in 1989. During this event, the Grid collapsed due to high MVAR flows [6] and elsewhere damage to transformers was reported in the continental US.

This project investigates a method to minimize the flow of GIC through power transformers. Literature on protection of transformers during GIC [7-11] has proposed grounding the neutral point of transformers through a capacitor, to block the flow of the quasi-DC GIC. The solution examined in this report entails inserting a capacitor between the earth and the neutral point of a power transformer when GIC is detected. Although the use of a grounding capacitor limits the flow of DC current through the transformer, an excessive voltage could buildup across the capacitor during ground faults and result in ferroresonance conditions. Thus some mechanism to control the neutral voltage rise needs to be incorporated into the solution. The investigation presented in this report examines the effectiveness and impacts of a GIC blocking solution proposed by EMPRIMUS LLC through time domain simulations. All simulations are carried out using the PSCAD/EMTDC® software program [12].

2. Proposed solution for blocking GIC

Figure1 shows the method proposed by EMPRIMUS LLC for transformer ground mitigation. The switch shown in Figure 1 for normal operation (over 99.8% of the time) is closed providing a near short to ground, hence the registered mark SOLIDGROUND™. The switch is opened when flow of GIC is detected. The presence of GIC is detected by monitoring the DC component in the ground current and the harmonic level (THD) in the transformer voltages. The opening of the breaker (DC Disconnect Switch & Grounding Switch in series) inserts the capacitor between the earth and the transformer neutral point, blocking the quasi DC GIC current. The DC Disconnect Switch used in the grounding circuit is expected to be able to break DC currents. The capacitor must be able to withstand the expected maximum ground fault voltage. Some form of overvoltage protection must be provided to avoid high neutral voltages during a ground fault that may occur when the capacitor is in the grounding circuit.

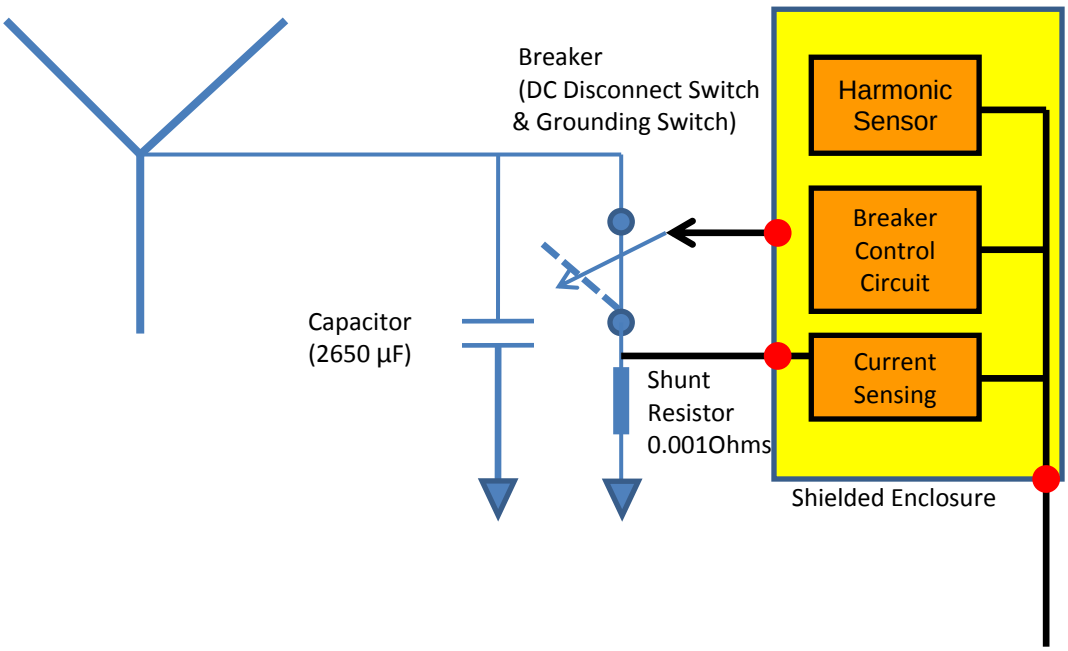

Figure 1: GIC mitigation method proposed by EMPRIMUS

3. Test network and the simulation model

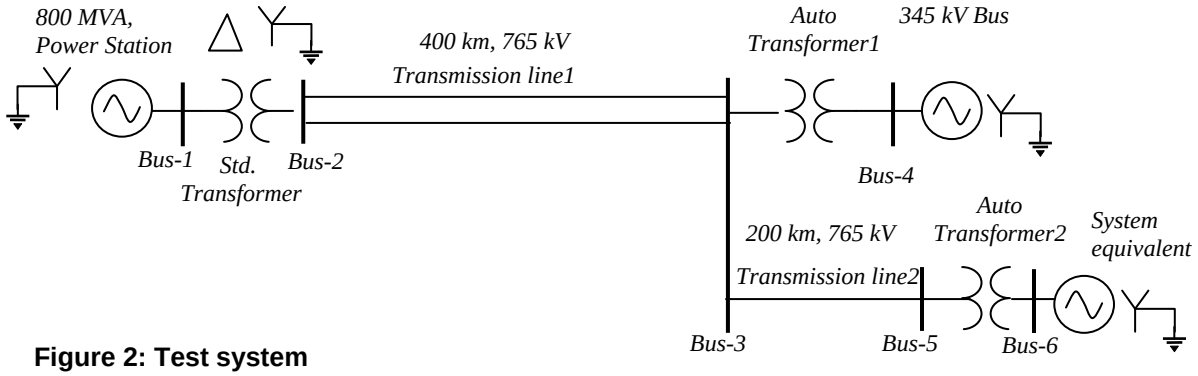

Figure 2: Test system

The structure of the test system used for the simulation study is shown in Figure 2. The three sources connected to buses 1, 4, and 6 represent system equivalents: the source connected to bus-1 represents a 800 MVA power station and the sources connected to buses 4 and 6 represent the networks beyond those buses that include transmission lines, transformers, loads, etc. They were simulated using the three-phase source model in PSCAD/EMTDC® master library. The source model used can accommodate different positive and zero sequence impedances. The initial values of the source voltages and phase angles were adjusted to maintain the required power flow.

Transmission lines were modeled using frequency dependent models that accurately simulate the high frequency behavior and coupling effects. A ground resistivity of 100 Ω.m (typical for flat terrain with fertile soil/marshy land [13]) was considered in modeling the transmission lines. In this study, line compensation reactors were connected in Delta configuration to avoid flow of GIC through them. Under practical situations, neutral of the compensation reactors may be grounded, and they would be affected by GIC in similar fashion to the autotransformers.

The transformers were modeled using the detailed transformer model available in PSCAD/EMTDC® master library. This model is capable of simulating AC saturation according to the characteristics specified by the user. This PSCAD/EMTDC® transformer model has been widely used to simulate phenomena such as inrush currents, where half cycle saturation of the core is involved. Although this transformer model in the PSCAD/EMTDC® master library does not model the hysteresis in the magnetic core, it is accurate enough to demonstrate the proposed mitigation concept. Neglecting of hysteresis in the simulations can somewhat affect the harmonic levels and the reactive power losses in the transformers. Very accurate simulation of these quantities is not essential to demonstrate the proposed mitigation concept. The important parameters of the test system are given in the Appendix.

Faults were simulated using the fault model available in PSCAD/EMTDC®. This model can be used to simulate different types of faults (ground, phase,-to-phase, three-phase) with different fault impedances. The timing of the faults can be set by the user.

Most previous studies have used injection of current sources to simulate flow of GIC. This approach is not suitable to study mitigation against GIC, thought it is effective when studying the influence of GIC on the transformers. When breaking an existing GIC path in the network, the current source model would attempt to force its current through an alternative path. For example

current could be forced through an open breaker that is modeled as very large impedance, creating spurious voltages in the simulation.

The cause for flow of GIC is the earth surface potential, and therefore, it is more appropriate to directly model the earth surface potential as voltages acting across the transformer neutral points. In order to facilitate this representation, a local ground bus was introduced at each of the substations, and the earth surface potential differences were modeled as slowly varying voltages injected between the true circuit ground and the local substation grounds. The relative magnitudes of the injected voltages (using controlled voltage sources) at the local grounds were adjusted considering distance between the substations. All voltage measurements were made with reference to the local grounds.

4. Modeling and simulating the mitigation concept

The model of the grounding circuit was constructed in PSCAD/EMTDC using the standard components available in the master library as shown in Figure 3. A neutral grounding capacitance of 2650 μF (equivalent to a 1Ω impedance at 60 Hz) was used at all three transformers.

The breaker (a DC Disconnect Switch and AC Grounding Switch in series) used in the grounding circuit is expected to be able to break DC currents. The voltage ratings of the commercially available DC Disconnect switches are lower than the neutral voltages expected during ground faults. The DC Disconnect Switch considered for this application has a voltage rating of 1,000 VDC. Thus this grounding switch is proposed to be constructed by connecting a DC Disconnect Switch in series with an AC High Speed Grounding Switch. Both the DC Disconnect Switch and AC Grounding Switch were simulated using the PSCAD/EMTDC breaker model, with different options. The AC Grounding Switch was modeled with “open possible at any current” option disabled and with a zero current chopping limit. The DC Disconnect Switch was simulated by allowing it to open at any current. The same trip signal was applied to both the DC Disconnect Switch & Grounding Switch.

The overvoltage protection for the capacitor during ground faults that may occur when the capacitor is in the grounding circuit is provided using an MOV. The MOV model available in PSCAD/EMTDC® master library was used for simulating a 5 kV MOV [14], with the nonlinear characteristics given in the Appendix.

The GIC mitigation design which includes the voltage harmonic sensor, current sensor, surge arrester and the breaker (the DC Disconnect Switch and AC Grounding Switch in series) control circuit was also implemented using the models available in the control systems library of PSCAD/EMTDC. Figure 4 shows a screenshot of the mitigation module as implemented in PSCAD/EMTDC simulation environment. The Fast Fourier Transform (FFT) component in PSCAD/EMTDC was used to estimate harmonics in the mitigation signals. The DC magnitude of the ground current was obtained by low pass filtering the measured ground current. This can also be obtained using the FFT component. The THD and the DC current component were compared against the threshold levels to determine the presence of any GIC events in the system. Time delays (0.5 seconds) were introduced to avoid malfunction during other events such as temporary faults, inrush current, etc.

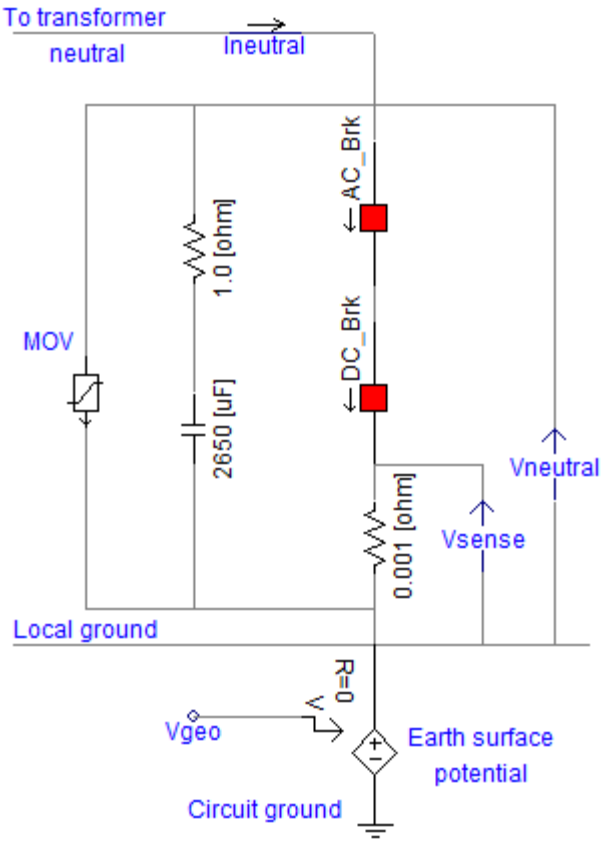

(a)

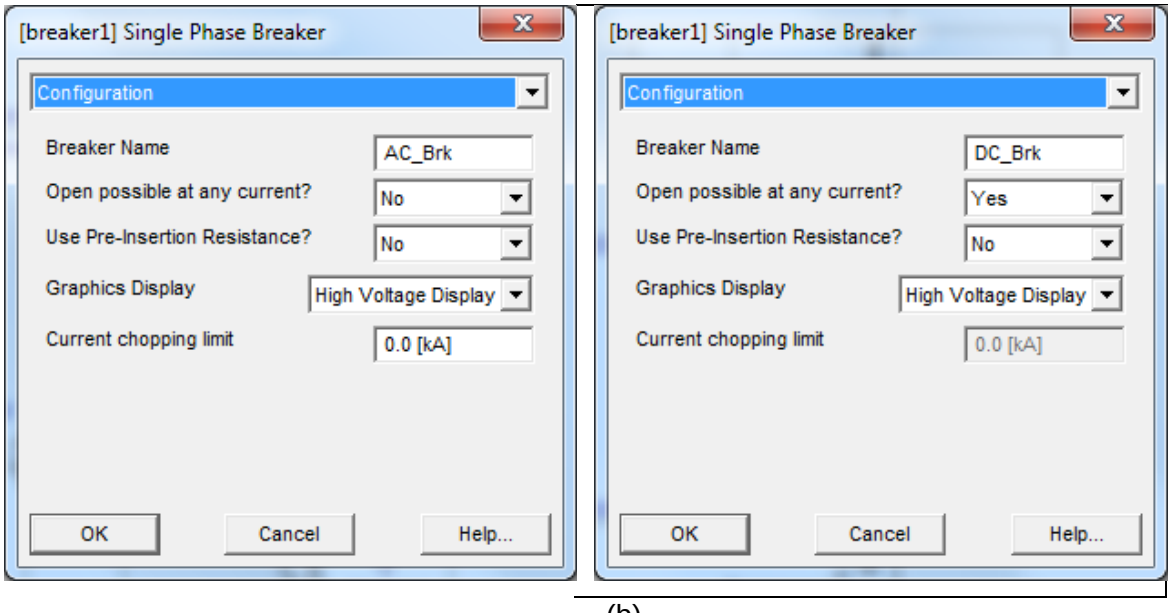

(b)

Figure 3: (a) PSCAD/EMTDC simulation model of the grounding circuit (b) Options for the AC Grounding Switch and the DC Disconnect Switches

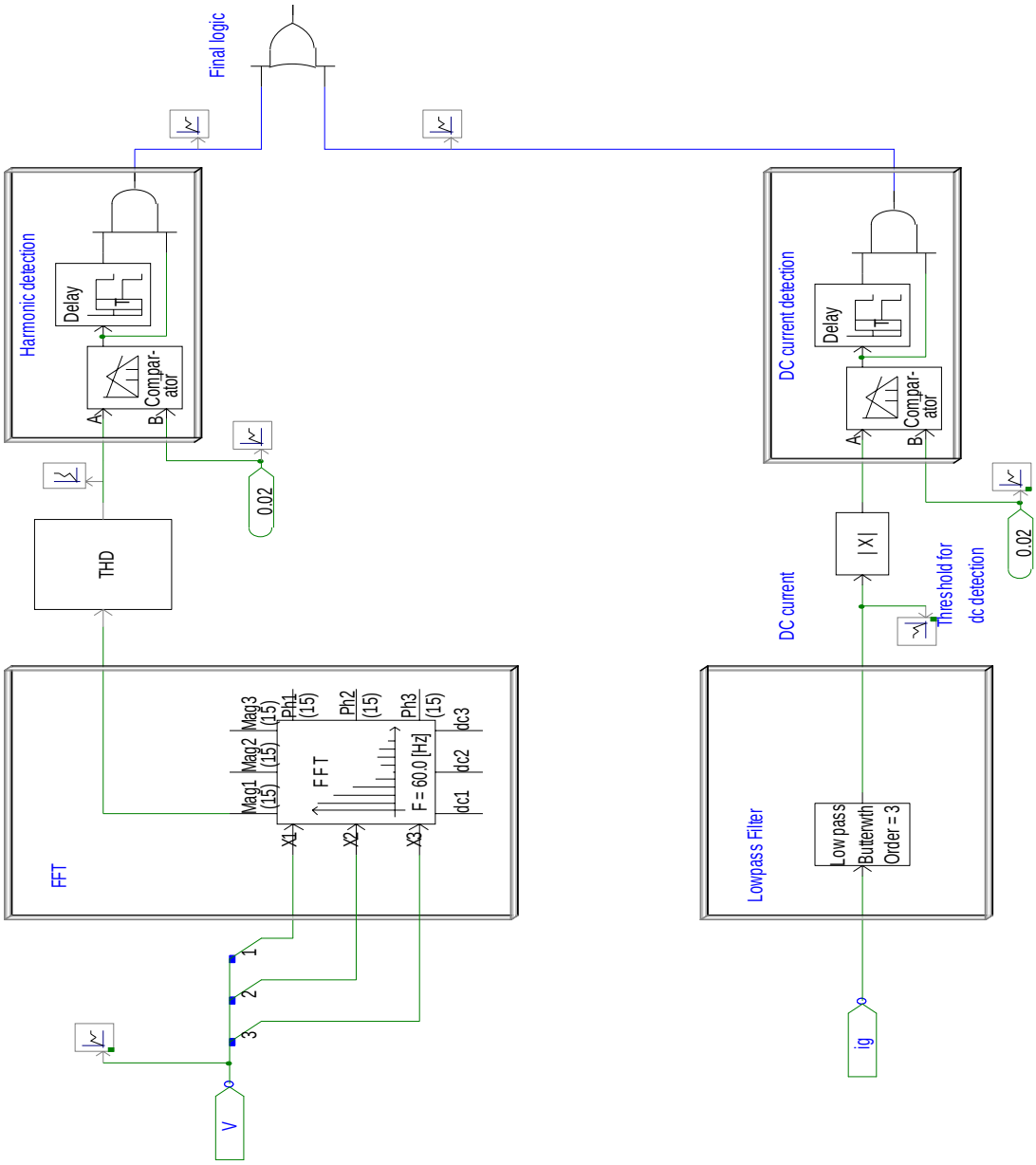

Figure 4: Implementation of mitigation concept

5. Simulation Studies

Behavior of the GIC mitigation design under different faults

In order to investigate the behavior of the GIC mitigation design under different faults and determine the proper settings (thresholds and time delays), variation of the ground current was investigated under different fault scenarios (ABC-G, A-G, A-B, AB-G, etc. at different locations) with no GIC flowing the network, i.e. with all voltages sources that represent the earth surface potentials having zero magnitude. Out of different fault types, the most concerned are the ground faults. An example simulation of phase A to ground fault on bus-3 (at the terminals of Autotransformer-1) are shown is shown in Figure 5. It was assumed that the transformer neutral is solidly ground (i.e. the AC Grounding Switch and the DC Disconnect switch are in the closed

position) at the time of fault. In Figure 5, variations of the ground current, DC component of ground current and the voltage THD observed at auto transformer T_1 during a temporary phase-A to ground fault (cleared after 0.1 s) are shown. For this fault, a ground current of over 20 kA rms was observed.

As it can be seen from Figure 5, the high level of harmonics is observed at the fault inception and clearing points, but the magnitude of THD quickly decays after the transient.

The slow variation of DC component in the ground current is due to time constant of the particular low pass filter used to extract the DC component. The DC component could alternatively be extracted through the FFT process, and this gives a faster response. The DC component calculated using FFT is also shown in Figure 5.

In order to avoid the operation of the proposed mitigation device due to the short term DC current and harmonics observed during temporary faults, a time delay (around a half second) can be introduced. This will also prevent the operation (malfunction) of the mitigation device due to transformer inrush currents observed during transformer excitation.

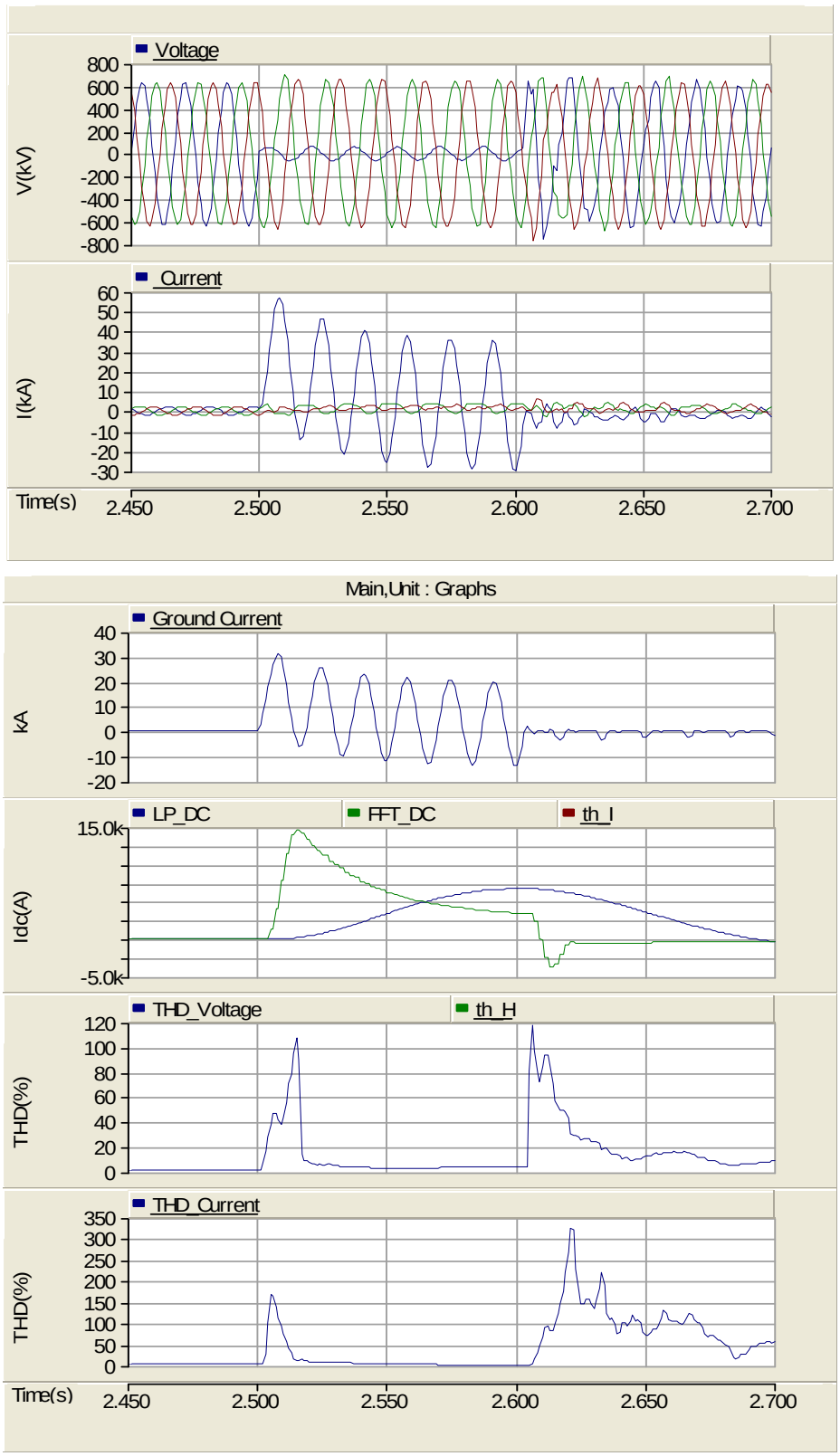

Figure 5: The transformer voltages, winding currents, ground current, DC magnitude of the ground current, voltage THD, and the current THD during a single line to ground fault at bus 3.

Effect of GIC on Transformer Operation

A GIC event was simulated and the behavior of the transformers without GIC mitigation during the disturbance was investigated. Figure 6 shows the variations of the injected earth surface potentials and the transformer neutral currents during a GIC event. Although the plots of the neutral currents appear as solid blue areas, they are sinusoids with varying magnitudes, rich in third harmonics as can be seen in the expanded view. The boundaries of each blue area represent the envelope of the sinusoidal signal. The GICs flow from the standard transformer to two auto transformers, since the earth surface potential at the standard transformer is higher than at the locations of the two autotransformers (as indicated by the relative magnitudes of the injected voltages).

The DC components of the ground currents and the transformer voltage THD variations during the GIC are shown in Figure 7. Although the DC current observed during the GIC events are not as high as the DC currents during faults, due to its continuing nature (slow variation) it may result in transformer saturation. This will ultimately result in increased reactive power consumption in the transformer.

The waveforms of the auto-transformer-1 current and voltage during the GIC event are shown in Figure 8. The simulated transformer current waveform is distorted more than the winding voltage waveform suggesting that the current THD could be a better indicator of GIC. However, since the load current can vary in a wide range during the operation, this may not be a good approach; the transformer current could have high THD value at no load or lightly loaded conditions, even without GIC. However, the total demand distortion, TDD, could be a potential alternative.

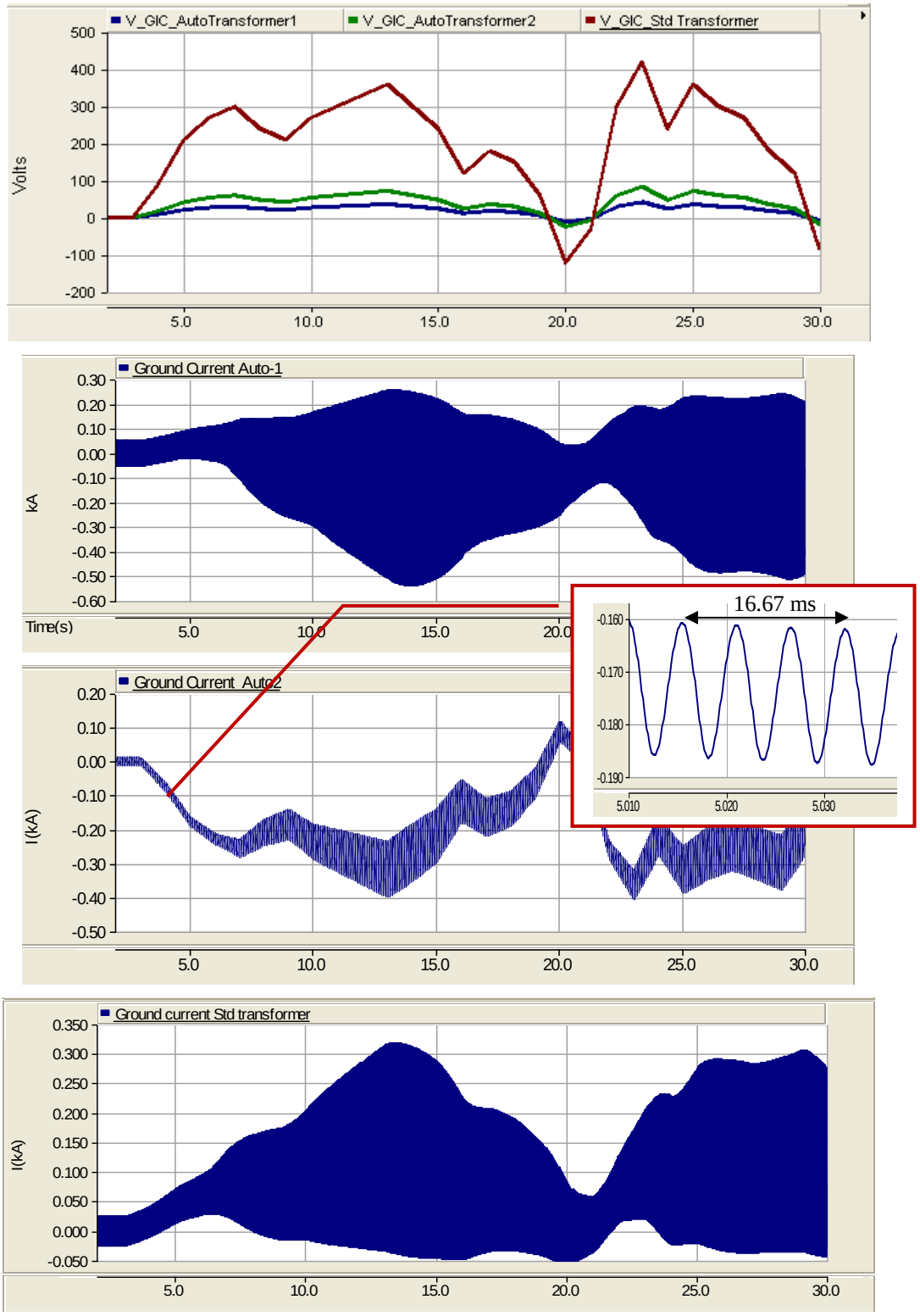

Figure 6: Injected surface potentials (blue: auto-transformer-1, green: auto-transformer-2, red: standard transformer) and variations of the transformer neutral currents during the GIC

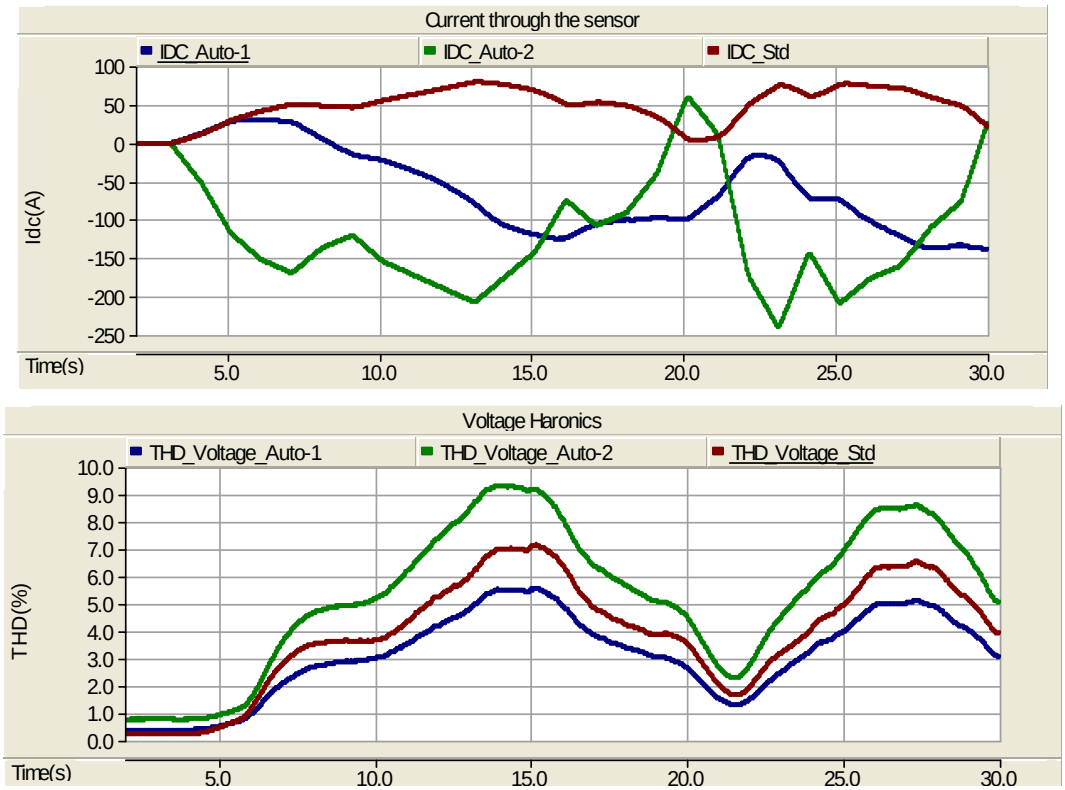

Figure 7: Variations of the of DC components of the transformer neural currents and THD of transformer voltages during the GIC event (blue: auto-transformer-1, green: auto-transformer-2, red: standard transformer).

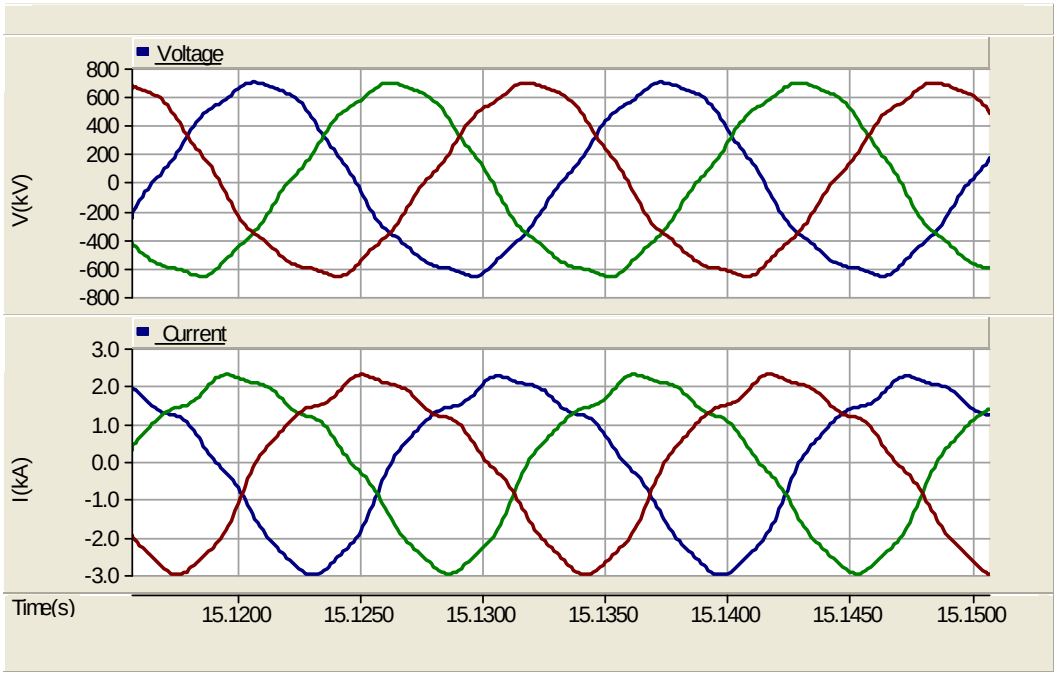

Figure 8: Auto-transformer-1 winding current and voltage waveforms during the GIC event.

Settings of the GIC Mitigation Design

In order to prevent the flow of GIC, the capacitor should be inserted in the transformer neutral grounding circuit. As explained before, flowing of GIC is detected by observing the DC component of the neutral current and the harmonic level of the transformer voltage. The settings are the threshold values of the DC component and the voltage THD. The thresholds must be set above the values of the respective variables observed under normal operation. Since these threshold values need to be made significantly smaller than the DC currents and the voltage THD values observed during the faults, a time delay must be introduced to discriminate between the faults and GIC. The following settings were used in the simulations presented in the next section.

Harmonic detection:

Threshold level: 2.0 %

Time delay: 0.5 s

DC current detection:

Threshold level: 20 A

Time delay: 0.5 s

Although a time delay of 0.5 s is considered in this study for demonstration of the concept, when applying to a specific power system, longer delays may have to be considered depending on the system specific features such as operation of auto-reclosers, single pole tripping, etc.

Operation of Mitigation Device during a GIC event

In this simulation, the GIC mitigation was allowed to operate automatically, that is whenever the DC component in the neutral current or the transformer voltage THD exceeded the respective thresholds, a signal is sent to open the breaker (the DC Disconnect Switch which in turn opens the Grounding Switch). It was observed that GIC mitigation at Auto-transformer 2 operated first, immediately followed by the GIC mitigation at the standard transformer and Autotransformer 1.

Figure 9 shows the variation of DC component of the neutral current, voltage THD and the operation of the mitigation device at auto-transformer 2 during the GIC event. In this simulation, the switches were opened due to high DC component in the ground current (> 20 A). However, due to time delay, the estimated DC current at the time that the switches opened was about 60 A. The voltage across the DC switch is well below its maximum operating voltage (1,000 VDC) at 40 A. The variations of the transformer neutral voltage and current are shown in Figure 10. The waveforms of the transformer winding voltage and current are shown in Figure 11. The corresponding observations at the other transformers are illustrated in Figures 12 – 17.

As it can be seen from Figures 9-17, opening of the grounding switches introduce high impedance to the paths of very low frequency GIC, effectively eliminating them. The residual values of the transformer neutral currents seen in Figures 10, 13, and 16 are much smaller than those seen in Figure 6. The operation of the mitigation device prevents the transformer saturation. Additionally, the GIC blocking configuration shown in Figure 1 does not introduce unwanted ferroresonance oscillations and overvoltages when the GIC mode is switched into operation.

Auto-transformer-2

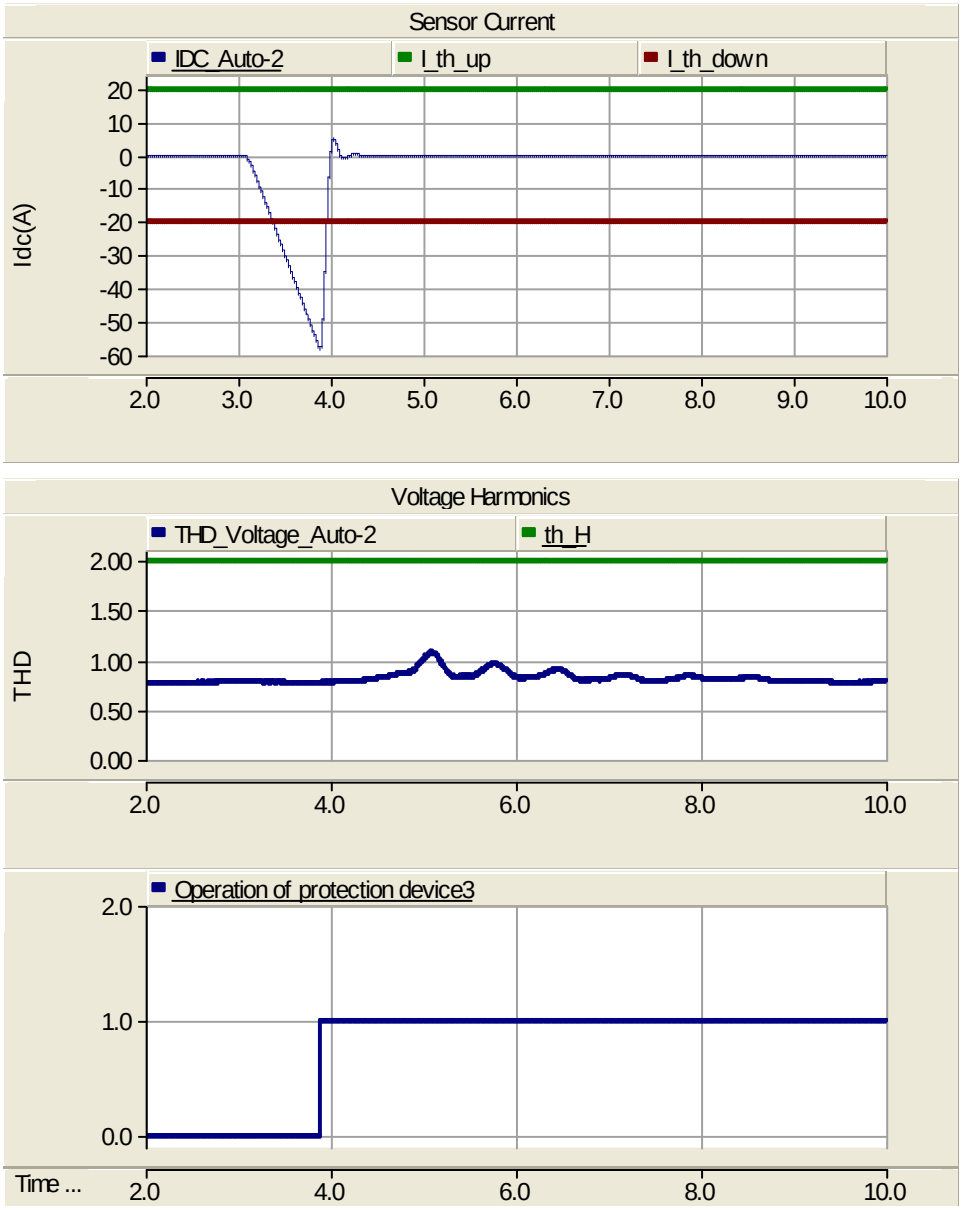

Figure 9: Variations of the DC component of the neutral current (A), voltage THD (%) and the operation of the mitigation device at Autotransformer-2 during the GIC event.

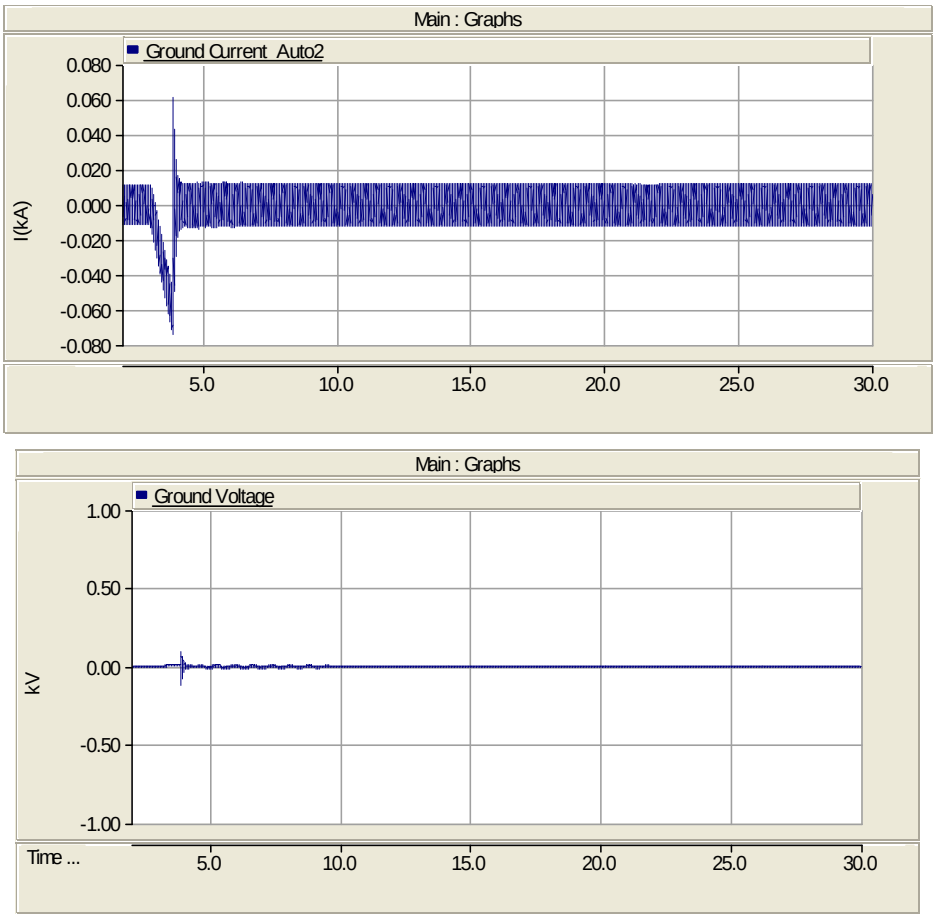

Figure 10: Variation of the Autotransformer-1 neutral current and voltage during the GIC event.

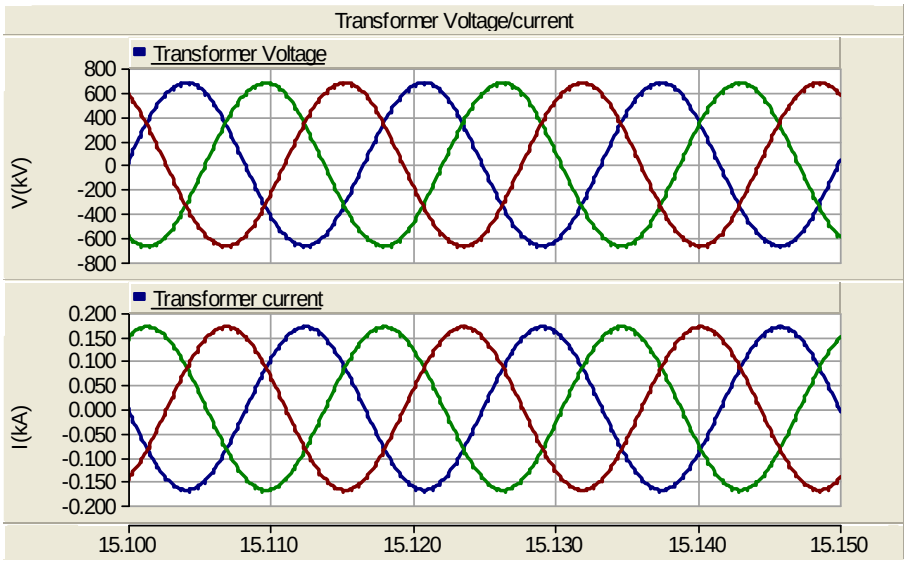

Figure 11: Autotransformer-1 winding voltage and winding current after the operation of GIC mitigation

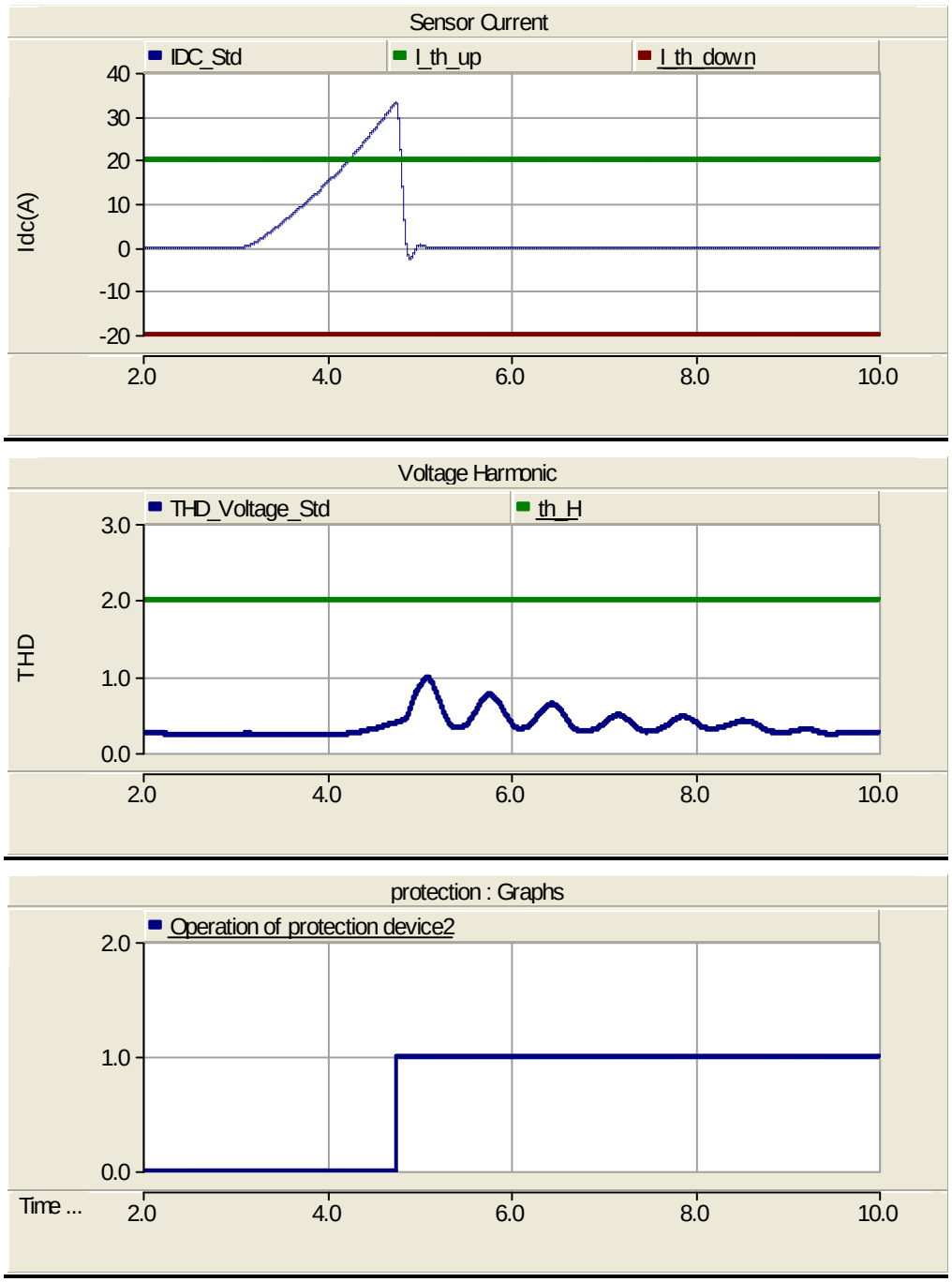

Figure 12: Variations of the DC component of the neutral current (A), voltage THD (%) and the operation of the mitigation device at the standard transformer during the GIC event.

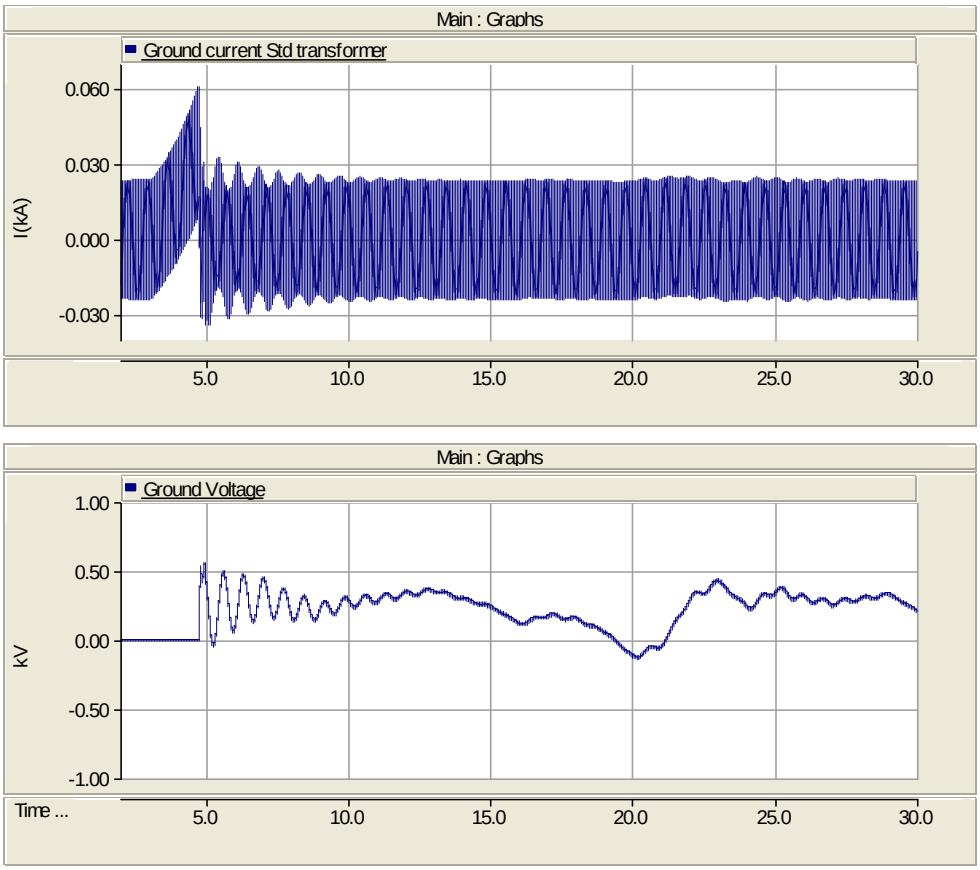

Figure 13: Variation of the Std transformer neutral current and voltage during the GIC event.

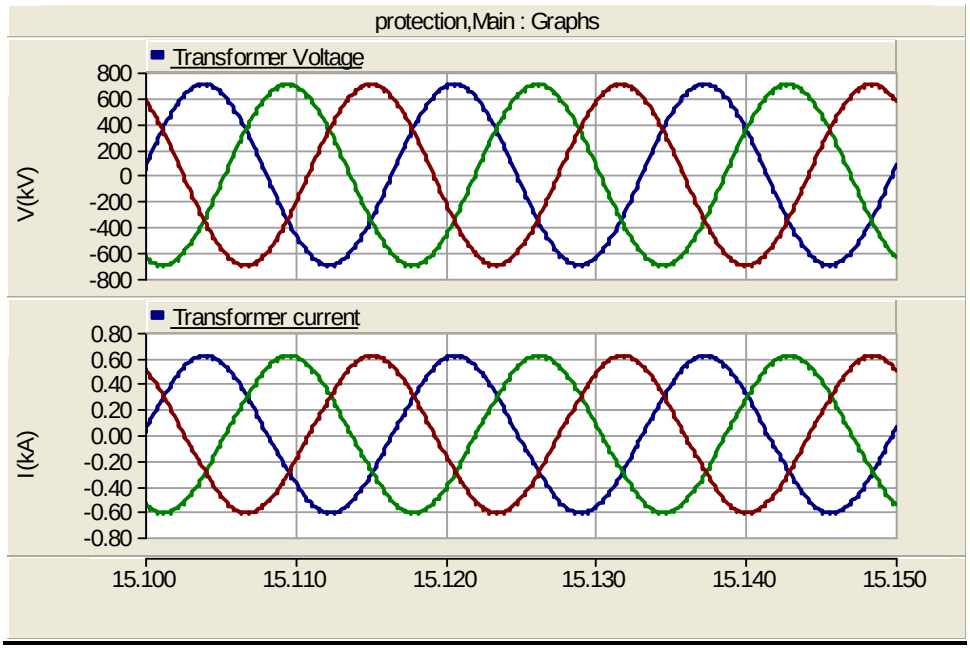

Figure 14: Std Transformer winding voltage and winding current after the operation of GIC mitigation

Auto-transformer-1

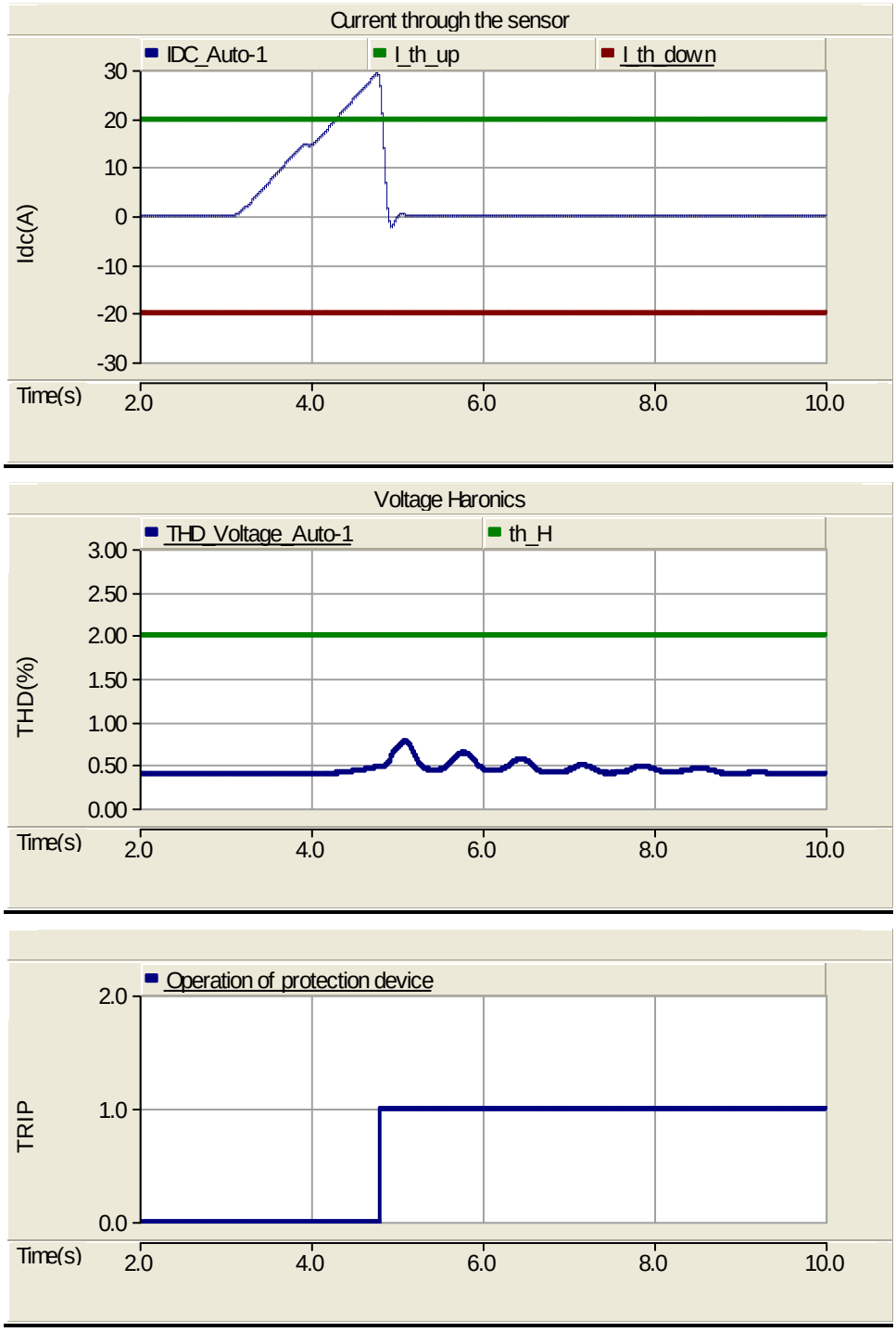

Figure 15: Variations of the DC component of the neutral current, voltage THD and the operation of the mitigation device at Autotransformer-1 during the GIC event.

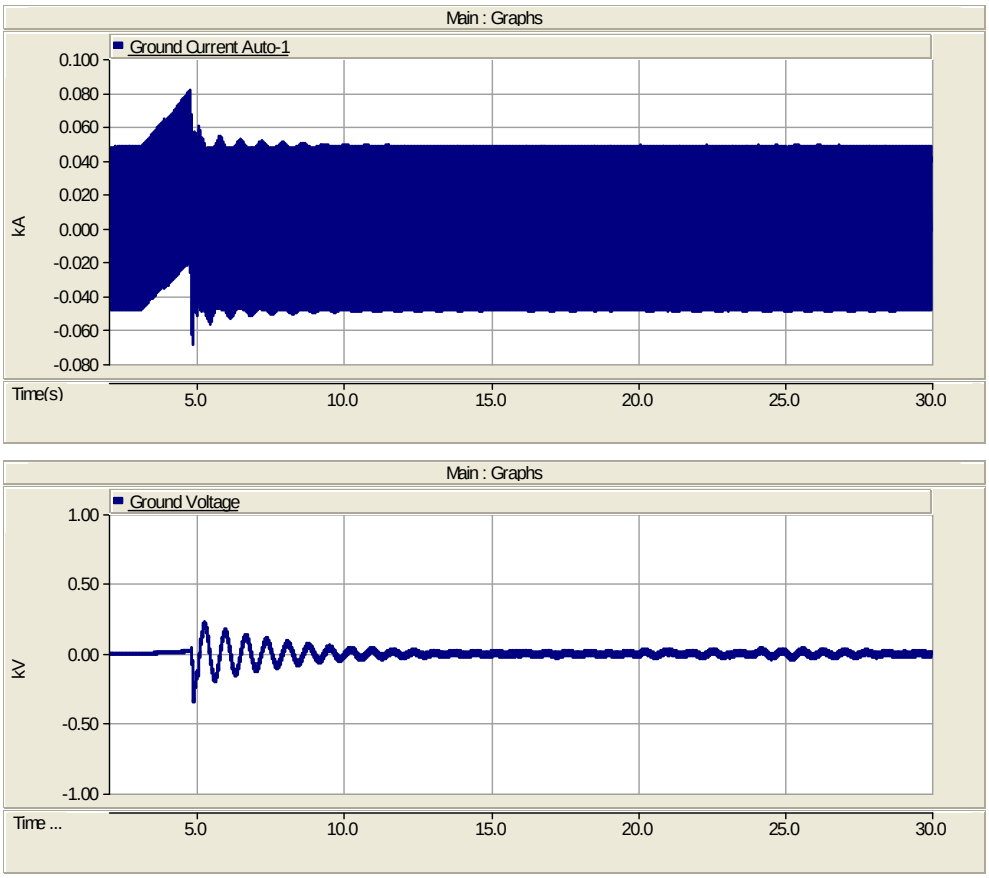

Figure 16: Variation of the Autotransformer-1 neutral current and voltage during the GIC event.

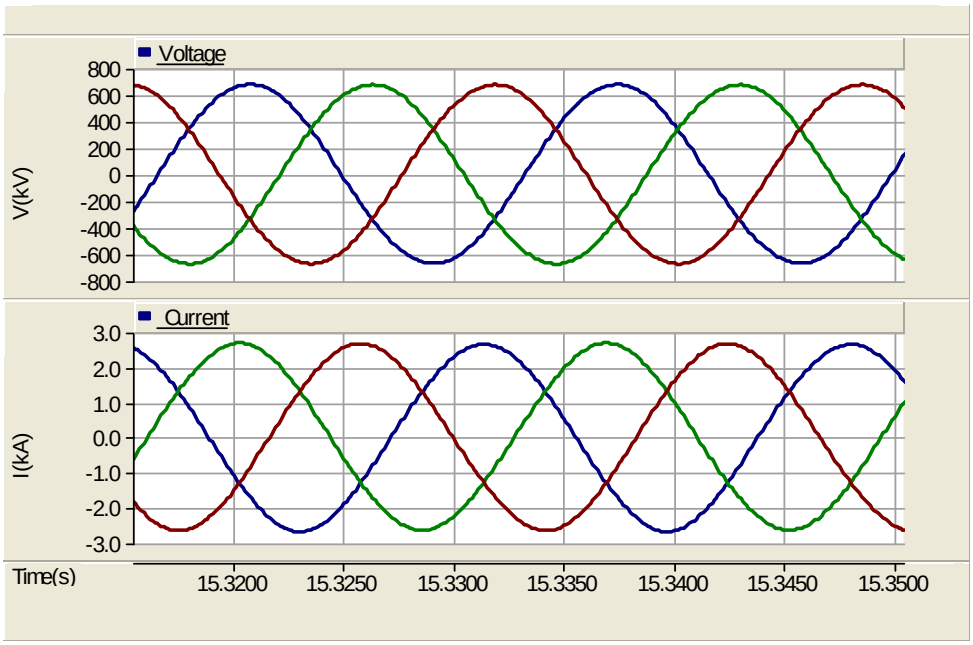

Figure 17: Autotransformer-1 winding voltage and winding current after the operation of GIC mitigation.

Impact of Change in GIC Potential

In order to investigate the robustness of the proposed method, a simulation was carried out using a higher injected voltage profile and a higher ground resistivity. Figure 18 shows the variations of the injected earth surface potentials and the transformer neutral currents during a GIC event without GIC mitigation. The DC components of the ground currents and the transformer voltage THD variations during the GIC are shown in Figure 19. The distorted waveforms of the auto-transformer-1 current and voltage during the GIC event are shown in Figure 20. In this simulation, a ground resistivity of 1000 Ω-m was used.

The waveforms after enabling the mitigation devices are shown in Figures 21-23. Figure 21 shows the variation of DC component of the neutral current, voltage THD and the operation of the mitigation device at auto-transformer 1 during this new GIC event. The variations of the transformer neutral voltage and current are shown in Figure 22. The waveforms of the transformer winding voltage and current are shown in Figure 23. As it can be seen from Figures 21-23, opening of the grounding switch, effectively eliminates the neutral DC current that causes transformer saturation, as in the previous case. This demonstrates the robustness of the SOLIDGROUND™ mitigation design when a higher ground resistivity and large GIC currents, up to 500 amps, are experienced.

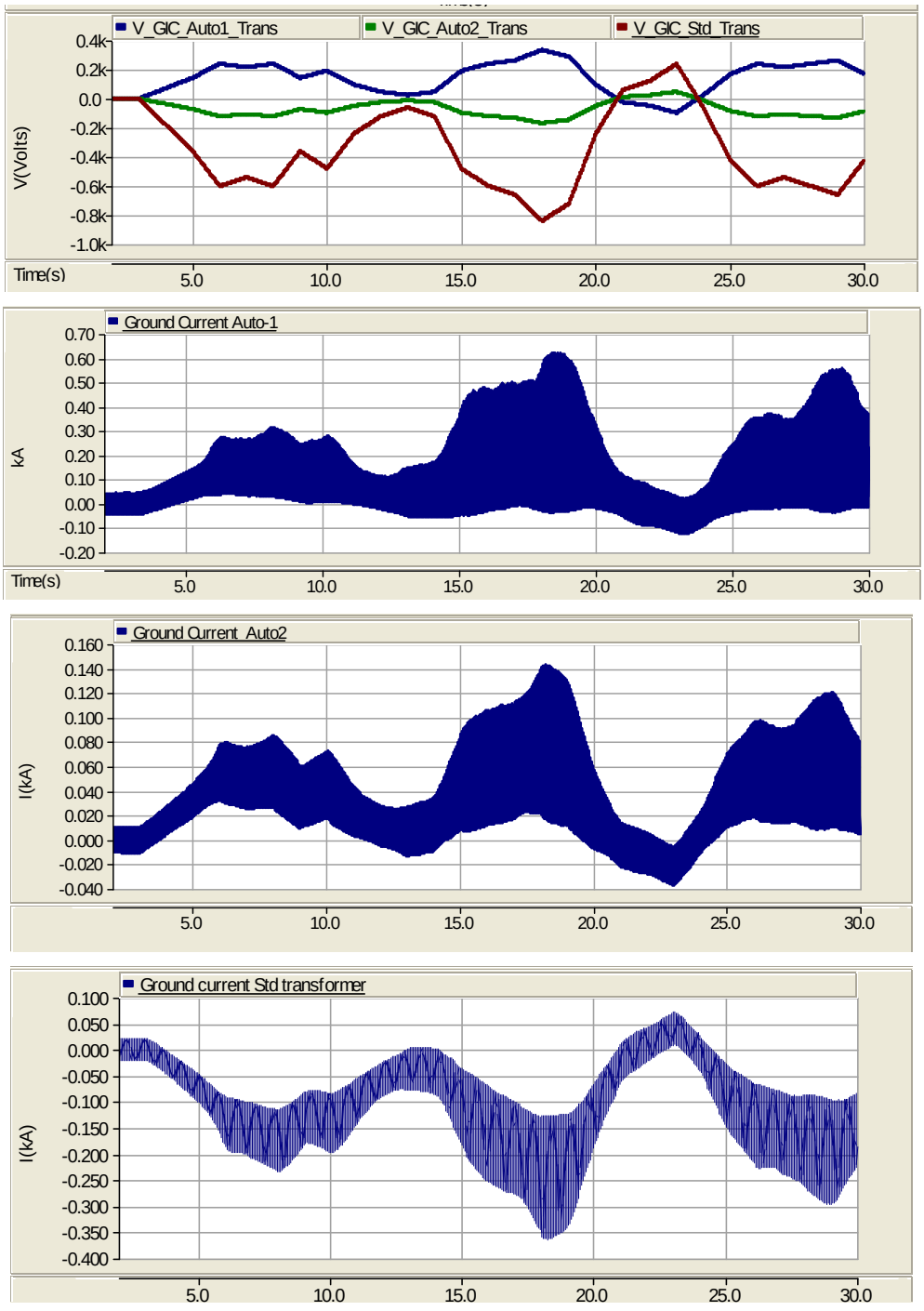

Figure 18: Injected surface potentials (blue: auto-transformer-1, green: auto-transformer-2, red: standard transformer) and variations of the transformer neutral currents during the GIC

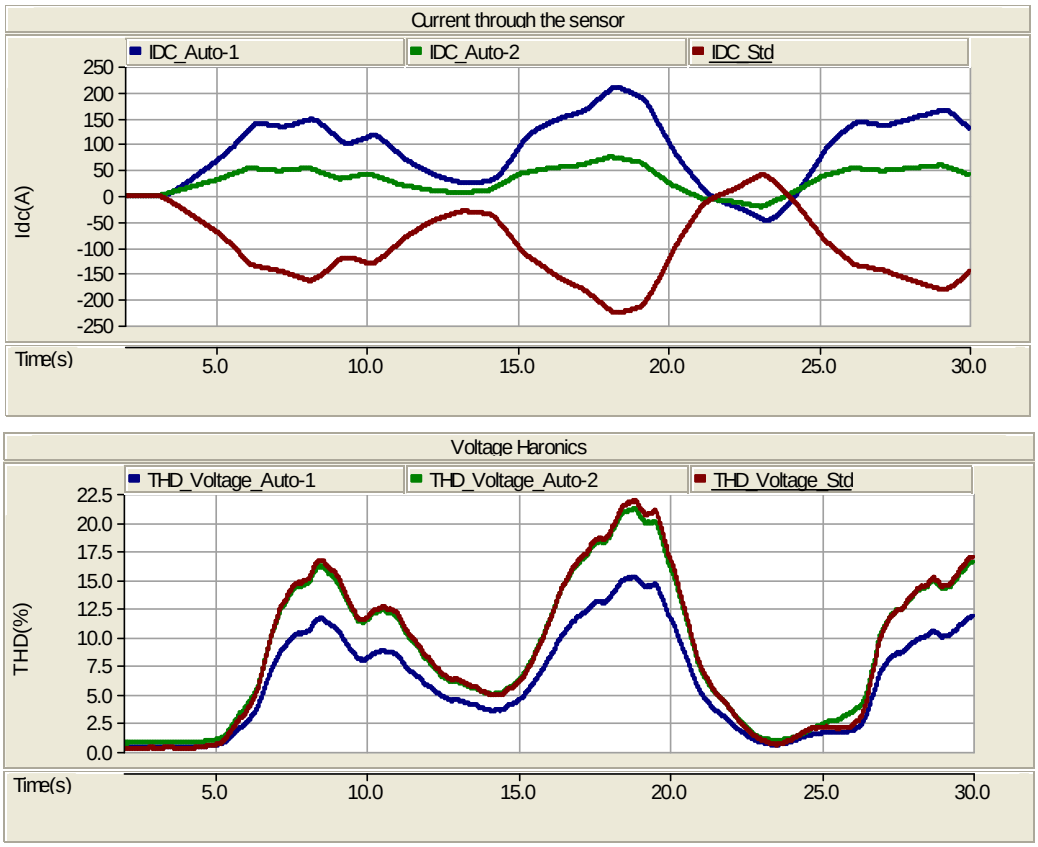

Figure 19: Variations of the of DC components of the transformer neural currents and THD of transformer voltages during the GIC event (blue: auto-transformer-1, green: auto-transformer-2, red: standard transformer).

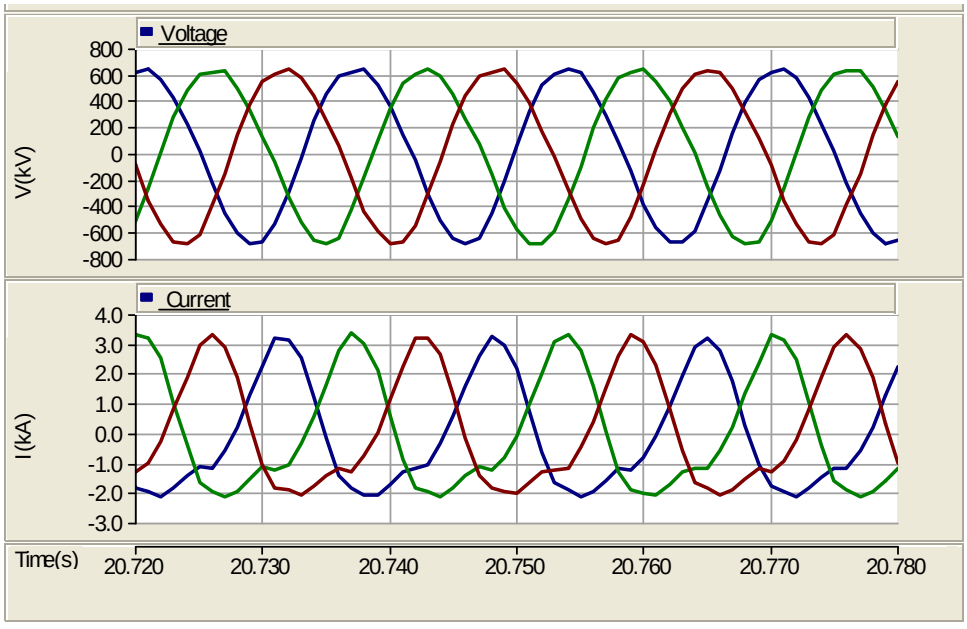

Figure 20: Auto-transformer-1 winding current and voltage waveforms during the GIC event.

Auto-transformer-1

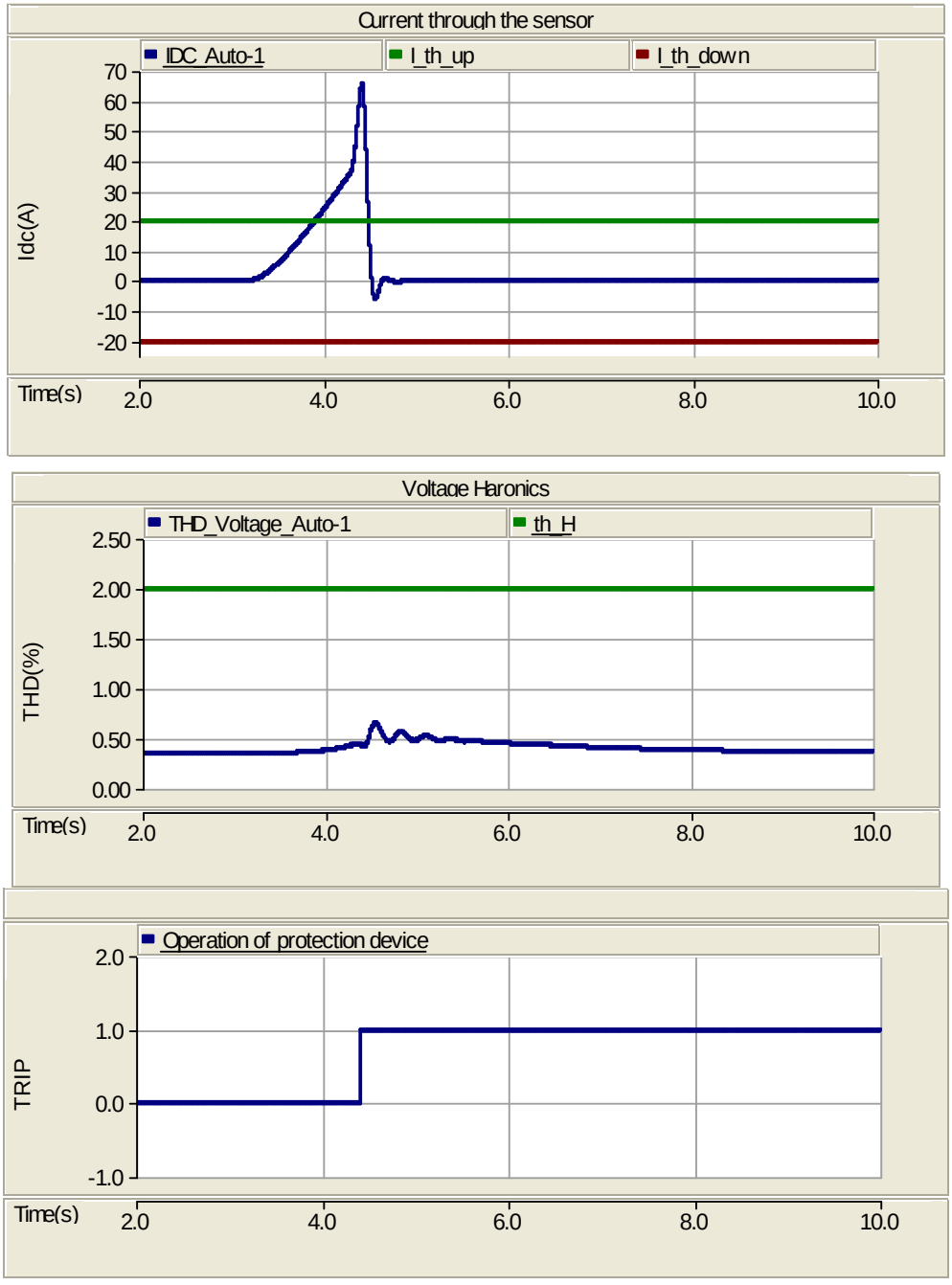

Figure 21: Variations of the DC component of the neutral current (A), voltage THD (%) and the operation of the mitigation device at Autotransformer-1 during the GIC event.

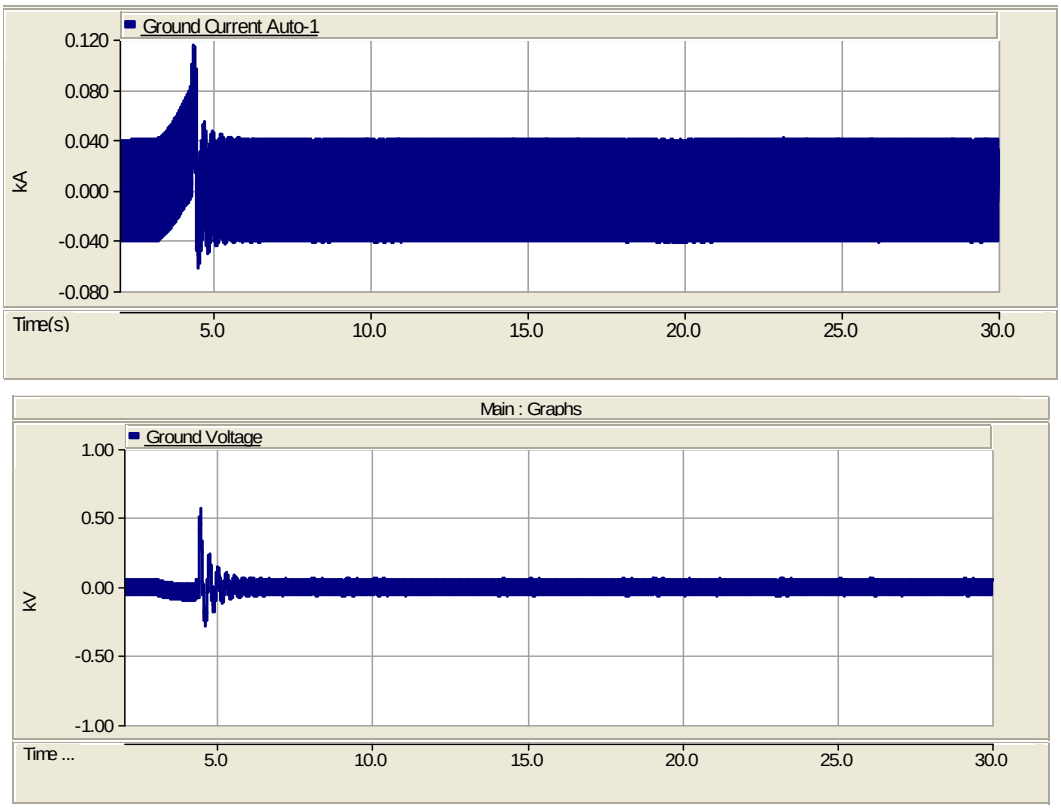

Figure 22: Variation of the Autotransformer-1 neutral current and voltage during the GIC event.

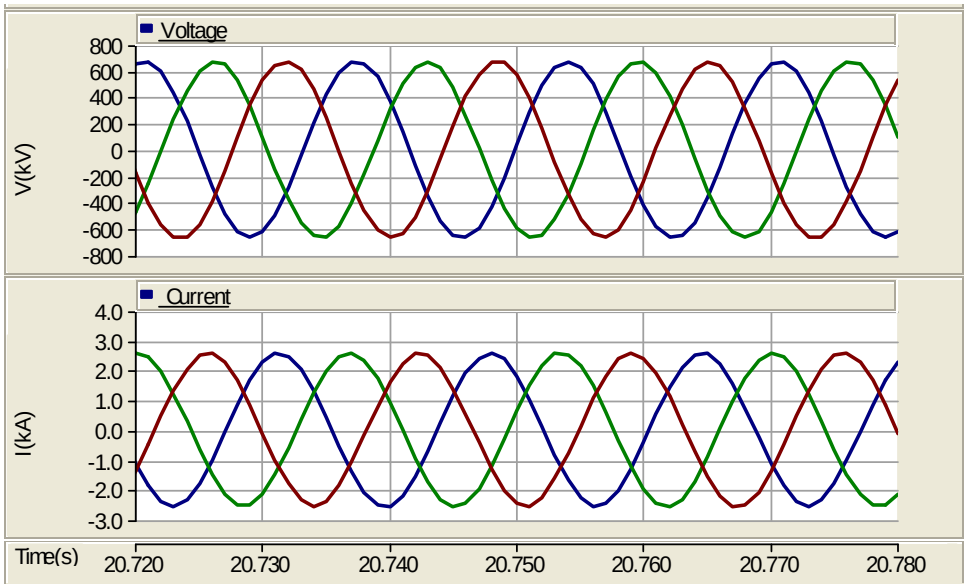

Figure 23: Autotransformer-1 winding voltage and winding current after the operation of GIC mitigation

Impact of Unbalanced Currents

In order to investigate the effect of unbalanced currents on the performance of the proposed method, transmission system was simulated using non-transposed transmission line models which results in some current unbalance in the system.

In this simulation, the GIC mitigation design was allowed to operate automatically, that is whenever the dc component in the neutral current or the transformer voltage THD exceeds the respective thresholds, a signal is sent to open the breaker (DC Disconnect Switch & Grounding Switch). The grounding switches at all transformers opened. The GIC protection at Auto-transformer 1 and the standard transformer operated first, followed by the GIC protection at the Autotransformer 2.

Figure 24 shows the variation of dc component of the neutral current, voltage THD and the operation of the protection device at Auto-transformer 1 during the GIC event. In this simulation, the breaker was operated due to high dc component in the ground current. The variations of the transformer neutral voltage and current are shown in Figure 25. The waveforms of the transformer winding voltage and current are shown in Figure 26. Figure 26 clearly shows an unbalanced current flow (approximately to 400 A) through the transformer.

Although the unbalanced current increases the third harmonics component in the neutral current, the proposed protection design operates based on neutral dc current and voltage harmonics (THD), no change in the operation can be observed due to the effect of unbalances current. Simulations were repeated for unbalanced loading conditions. Results showed no change in the operation.

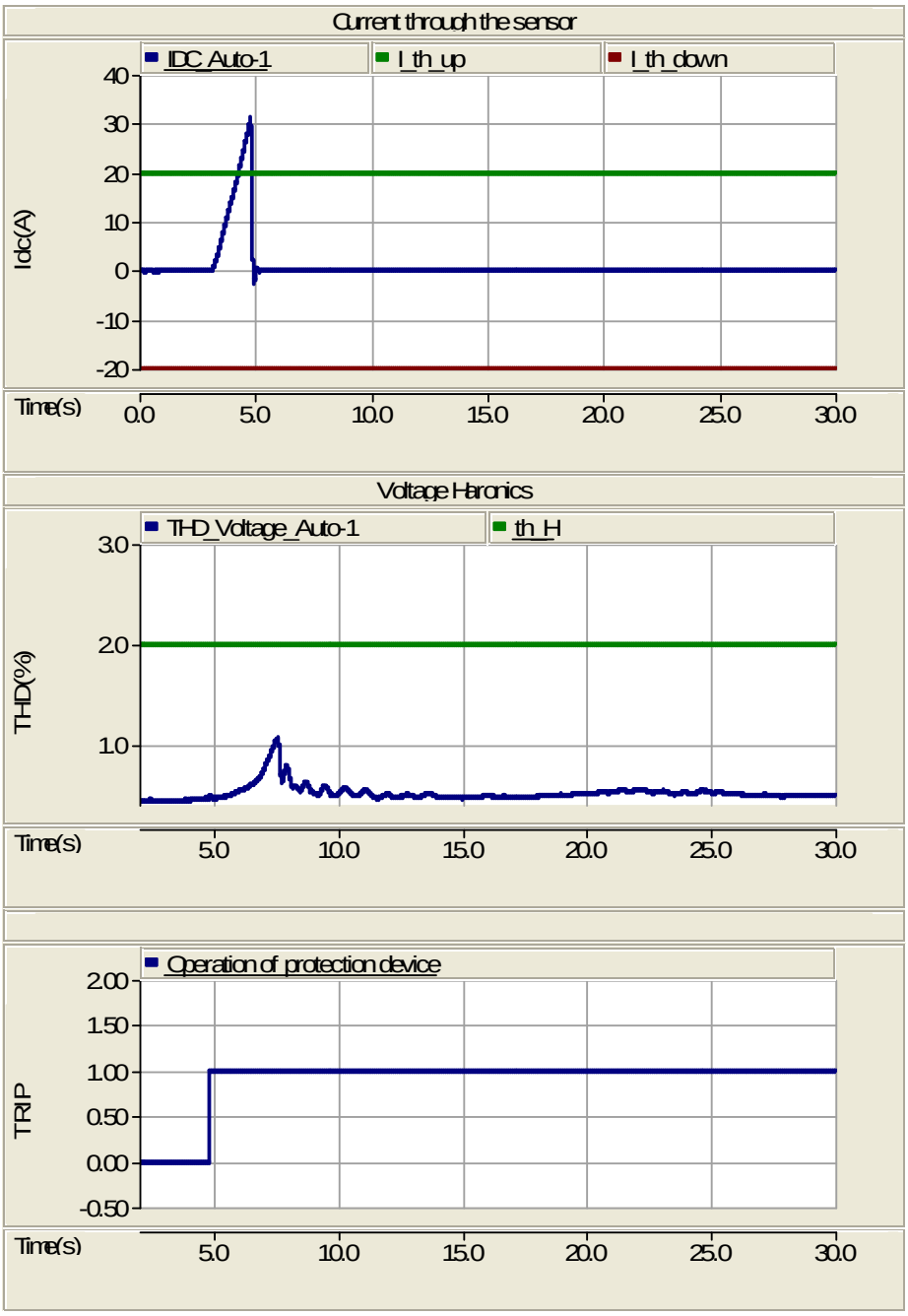

Figure 24: Variations of the dc component of the neutral current, voltage THD and the operation of the protection device at Autotransformer-1 during the GIC event.

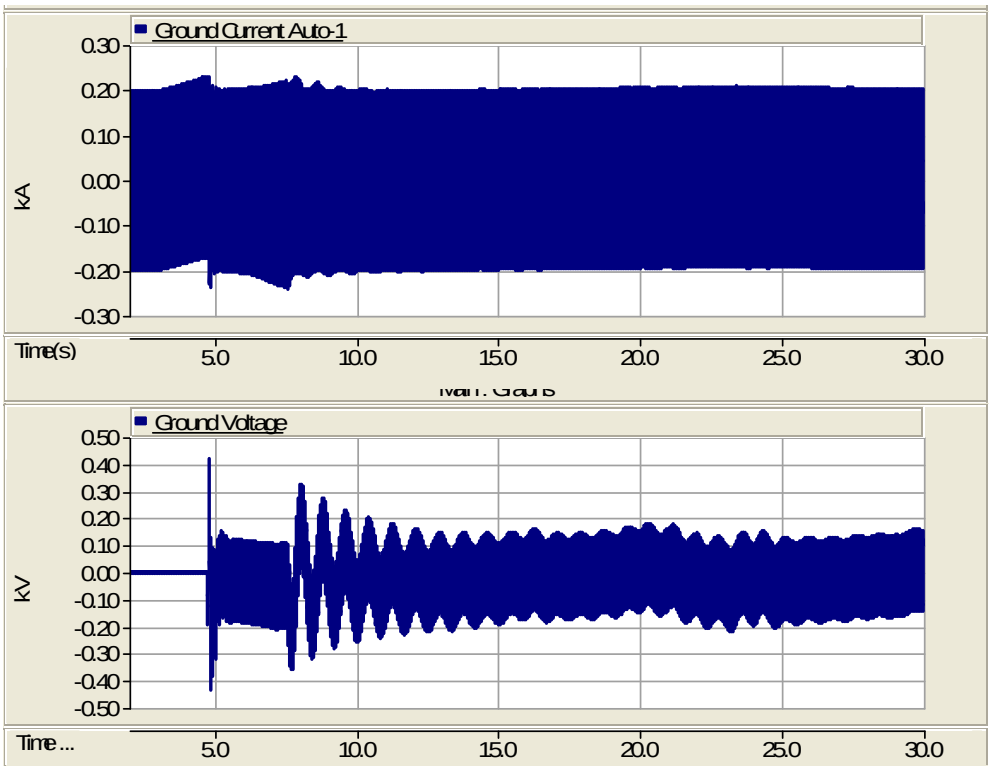

Figure 25: Variation of the transformer neutral current and voltage during the GIC event.

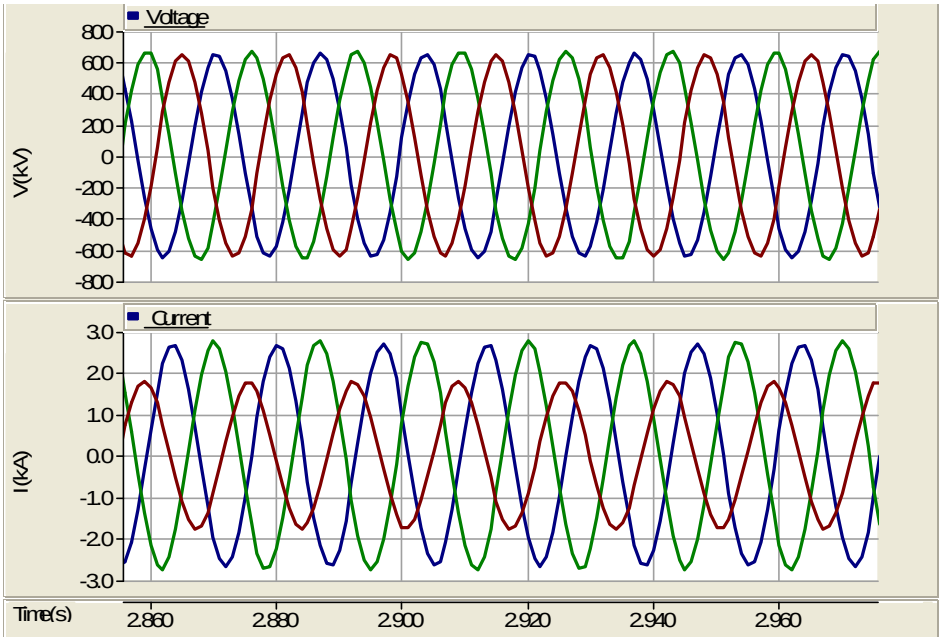

Figure 26: Transformer winding voltage and winding current after the operation of GIC protection

Impact of the GIC Mitigation on System Voltage and Neutral Voltage

The operation of the proposed mitigation design during ground faults could result in increased system voltages due to higher grounding impedance. In order to investigate this, simulations were carried out with MOVs removed from the grounding circuits.

Figure 27 shows the variation of phase C voltage (instantaneous values and rms values) on bus-5 during a phase A to ground fault at bus-2, with a transformer neutral grounding capacitance of 2650 µF. The fault occurs at 2.8 s and cleared at 2.9 s. The unfaulted phase rms voltage is highly oscillatory during the fault, indicating the possible existence of ferroresonance conditions. The simulations show an increase in the unfaulted phase voltages with the increase of grounding impedance (decrease in grounding capacitance).

Figure 28 shows the variation of neutral current and voltage at autotransformer-2, during the same ground fault.

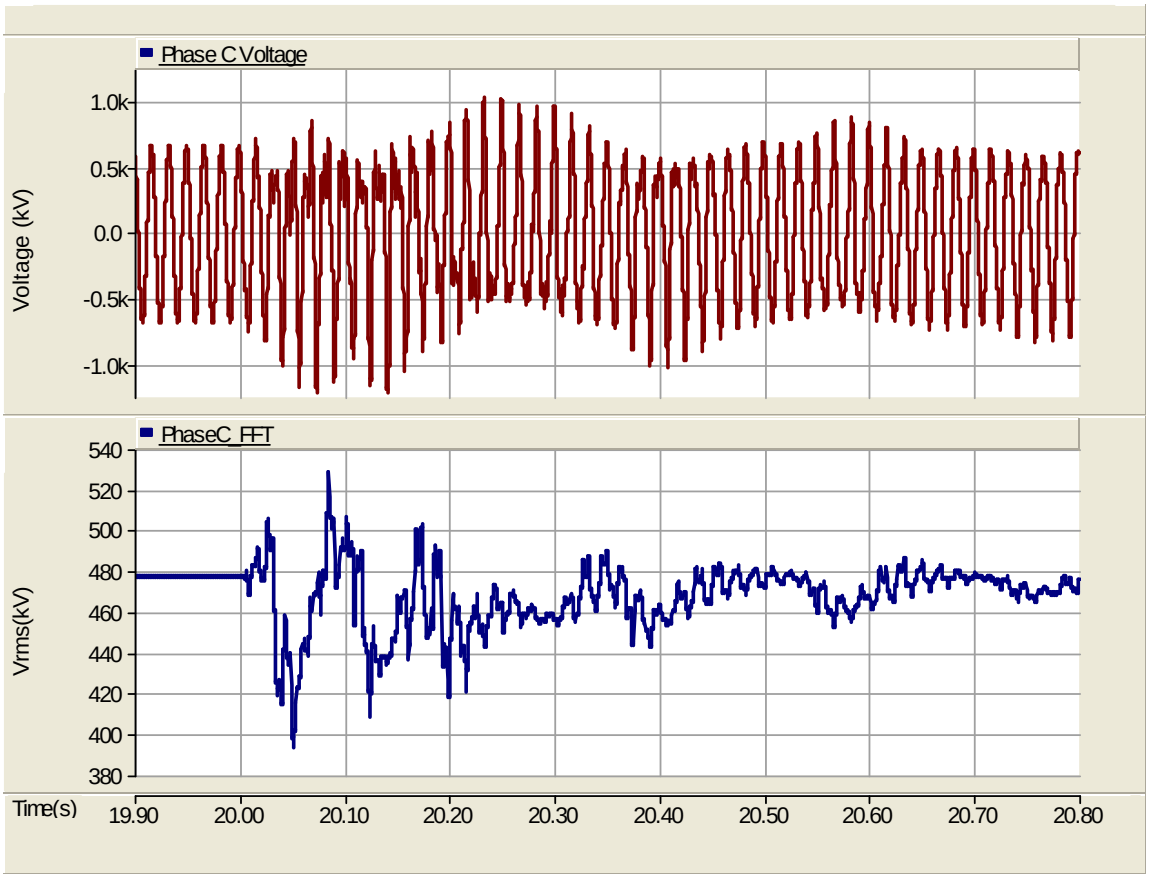

Figure 27: Variation of phase- C voltage on bus-5 during a line-to-ground fault on bus-2 for a grounding capacitance of 2650 µF

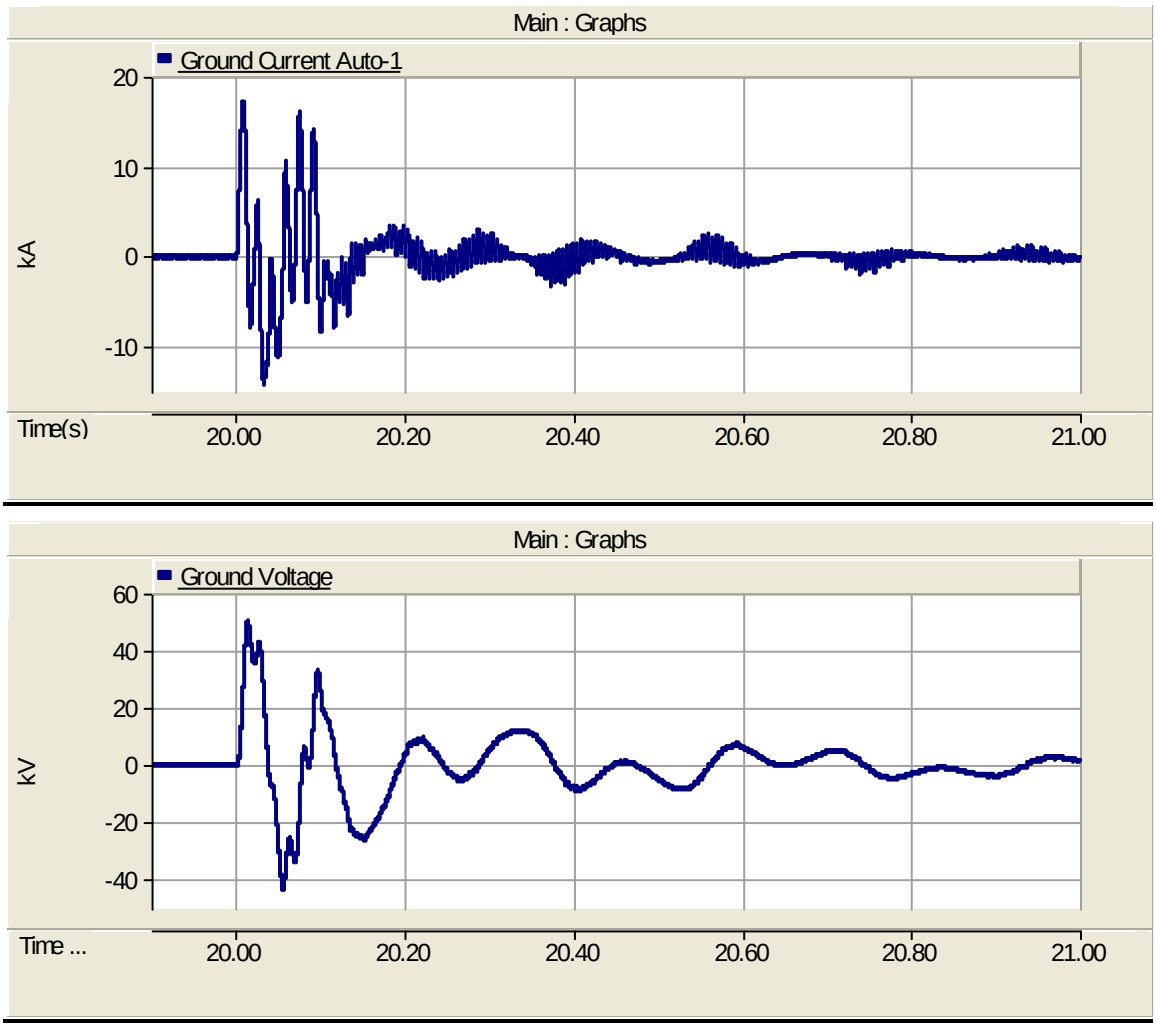

Figure 28: Variation of neutral current and voltage during the ground fault on bus-2.

The observed phase C voltage (instantaneous values and rms values) on bus-5 during phase AB-G fault simulated on the transmission line connecting buses-3 and 5 are shown in Figure 29. The fault was cleared in 0.1s. The corresponding variations of autotransformer-2, neutral current and voltage are shown in Figure 30.

The above simulations results show unacceptable overvoltages during the ground faults, if the capacitor was included in the grounding circuit.

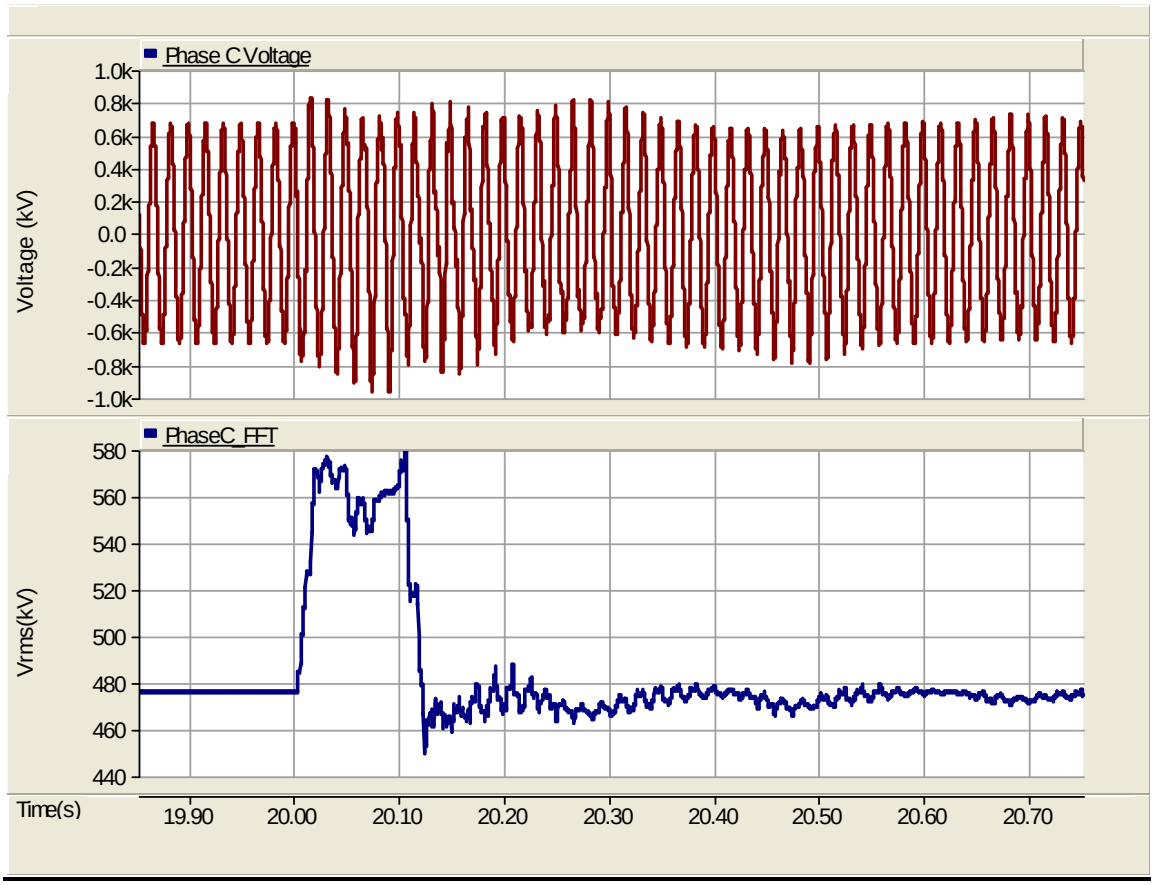

Figure 29: Variation of phase- C voltage on bus-5 during a line-to line-to-ground fault on transmission line connecting buses-3 and 5

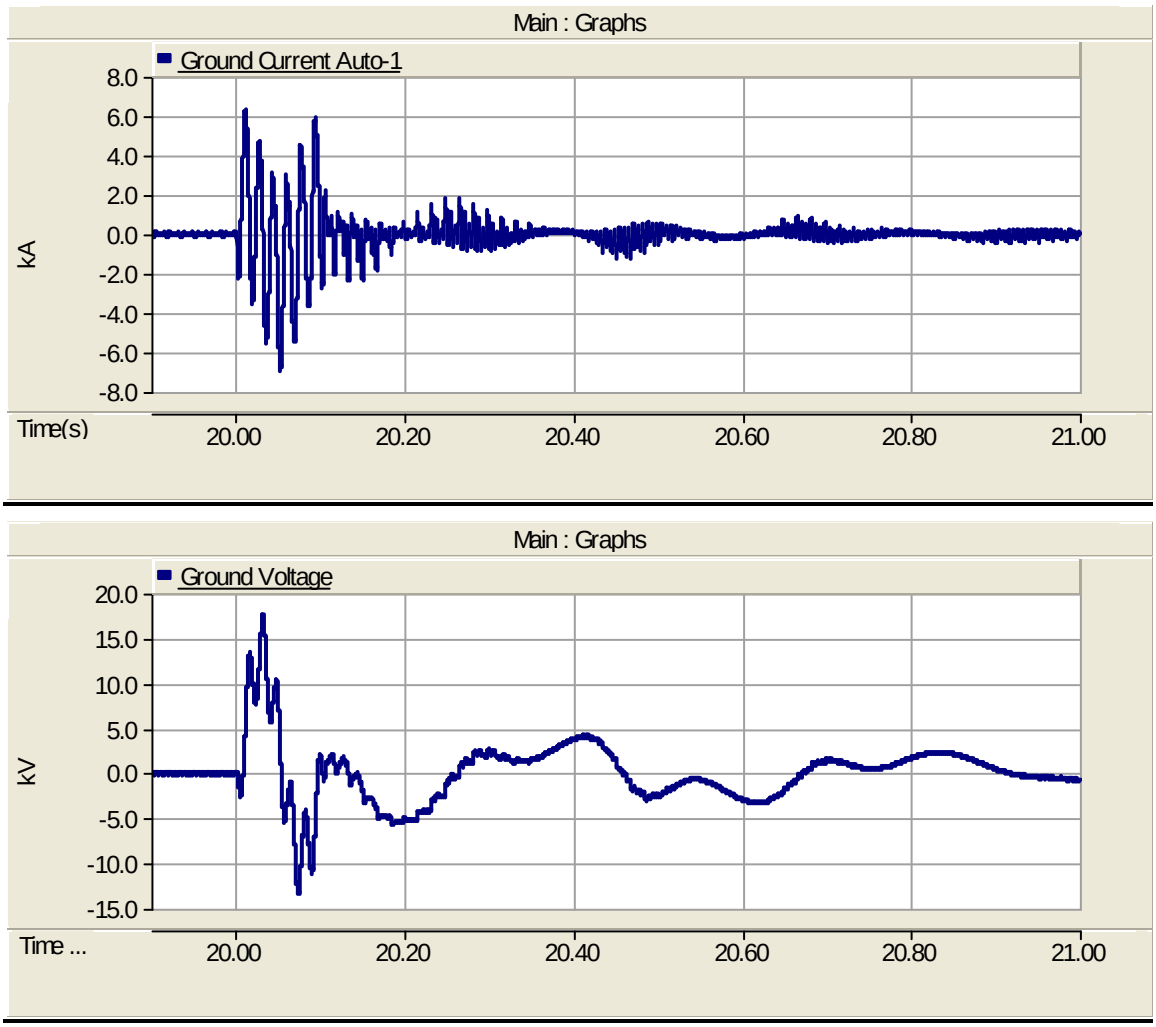

Figure 30: Variation of neutral current and voltage during the fault

Methods of Reducing Ferroresonance and High Neutral Voltages

Simulations were carried out to investigate the possibility of reducing ferroresonance conditions and high neutral voltages using different methods such as change of neutral capacitance, adding a series resistor and use of surge arrester. The simulation results obtained in this study are summarized below.

Effect of the value of grounding capacitance

In order to investigate the effect of increasing grounding capacitance, simulations were repeated with different capacitor values. The disturbance considered was the ground fault at bus-2. The variation of system voltage on bus-5, grounding voltage and grounding current of the autotransformer-1 are shown in Figures 31, 32 and 33 respectively.

As it can be seen from Figures 31,32 and 33, increase in capacitance from 2650 μF to 5300 μF results in a significant reduction in the oscillations in the system voltage, neutral current, and neutral voltage. There is a reduction in the overvoltages as well. Further increase of capacitance from 5300 μF to 7950 μF, resulted in an increase in oscillations in the system voltage and neutral voltage/current. However due to the increase of capacitance a reduction in overvoltages was observed.

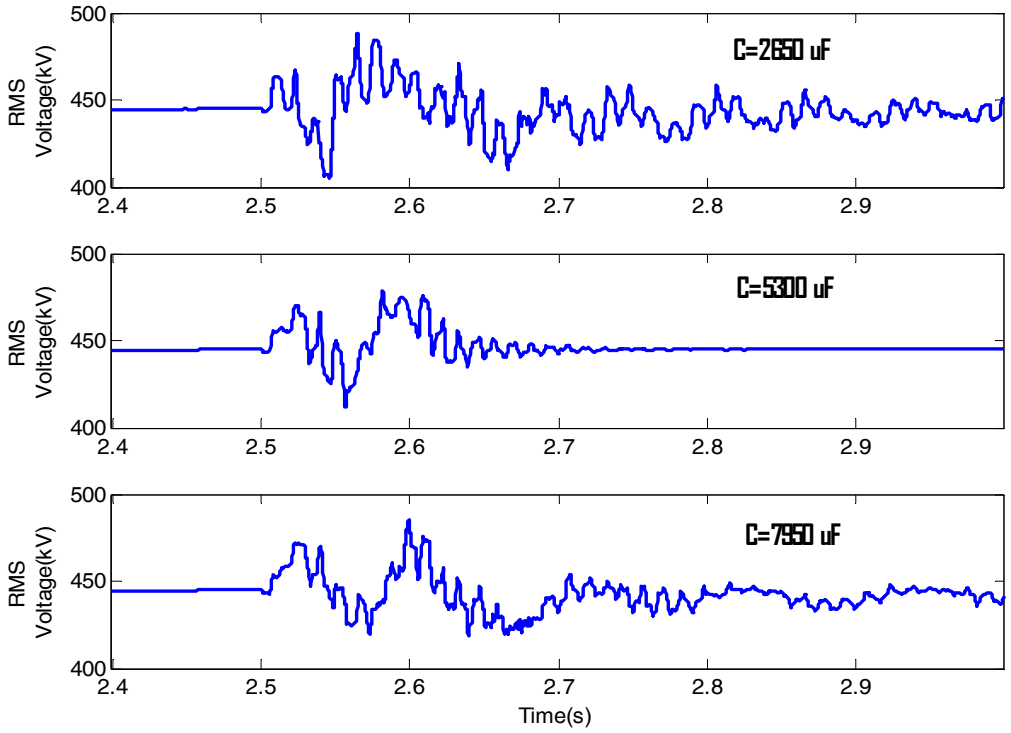

Figure 31: Variations of phase C (rms) voltage on bus-5 during a phase A to ground fault simulated on bus-2, with different grounding capacitances

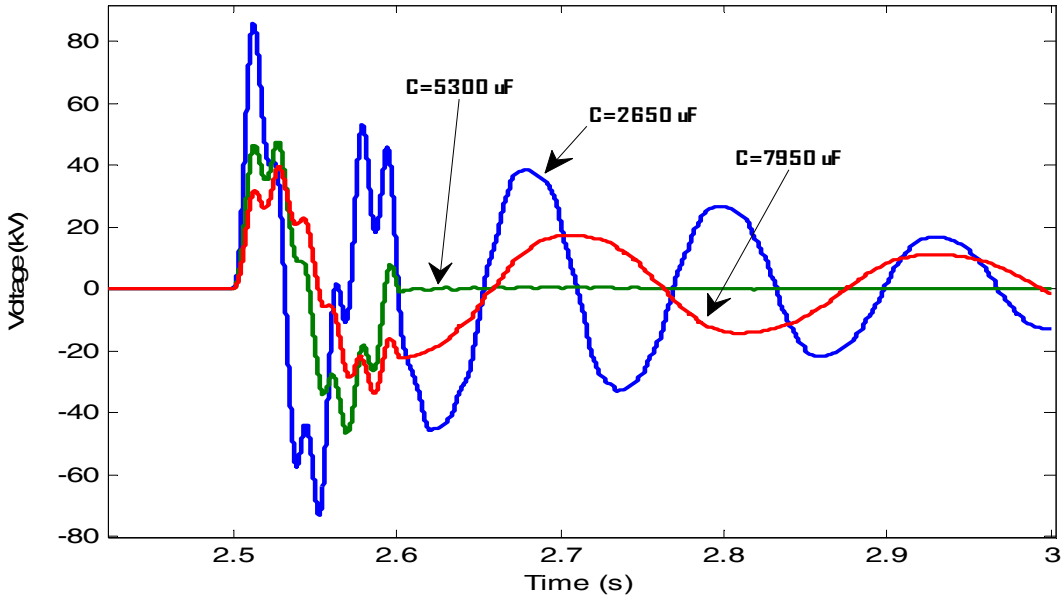

Figure 32: Variations of neutral voltage of autotransformer-1 with different capacitances during a phase A to ground fault simulated on bus-2,

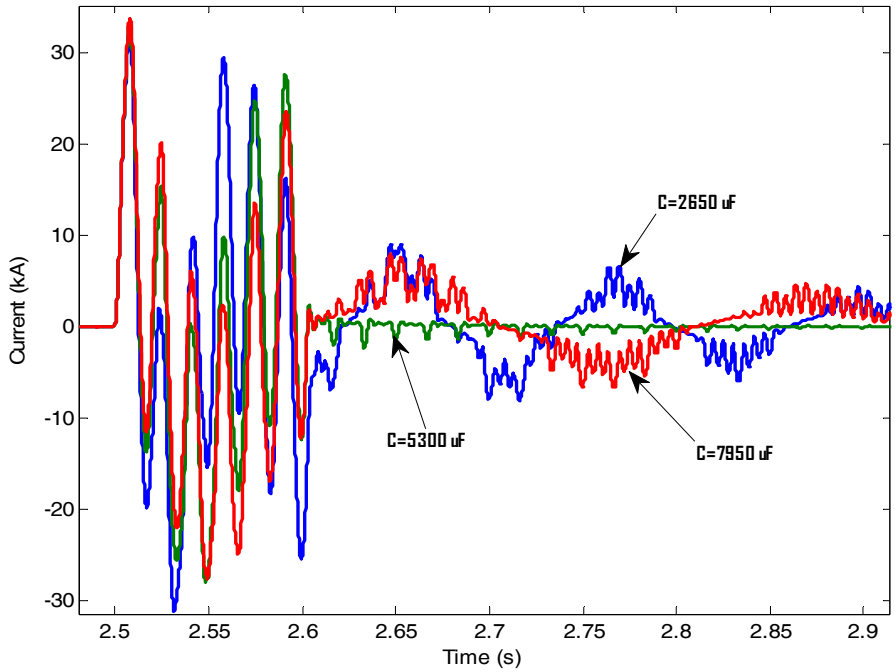

Figure 233: Variation of neutral current of autotransformer-1 with different capacitances during a phase A to ground fault simulated on bus-2,

Effect of Series Resistor

Ferroresonance and resulting overvoltages were observed during ground faults that occur while the transformer neutrals are grounded through capacitors. Simulations were carried out to investigate the impact of connecting a series resistor with the grounding capacitor on the ferroresonance. The GIC blocking design used for this study is shown in Figure 34.

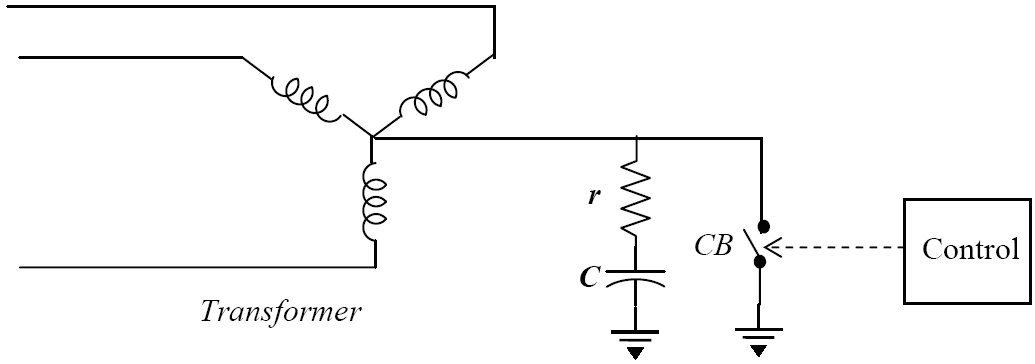

Figure 34: GIC blocking design with a resistance in series with the grounding capacitor

The scenario simulated is a ground fault on phase A at bus 3, while the circuit breaker CB (the Grounding Switch) in the grounding circuit is open. Simulations were repeated with different values for the resistance *r*. The resistance values considered was in the range of 0–5 ohms. The MOV was kept disconnected.

Figure 35 shows the variation of the rms value of phase C voltage on bus-5 during this fault. The corresponding variations of the neutral current and the neutral voltage of the autotransformer-1 are shown in Figures 36 and 28 respectively.

The results of this study show that, adding a resistance in series with the capacitor helps to reduce the oscillations observed in the neutral voltage. A resistance of about 5.0 ohms is required to completely remove the ferroresonance oscillations for this particular case. However, such high level of resistance causes a higher transformer neutral voltage, as well as a higher healthy phase voltage.

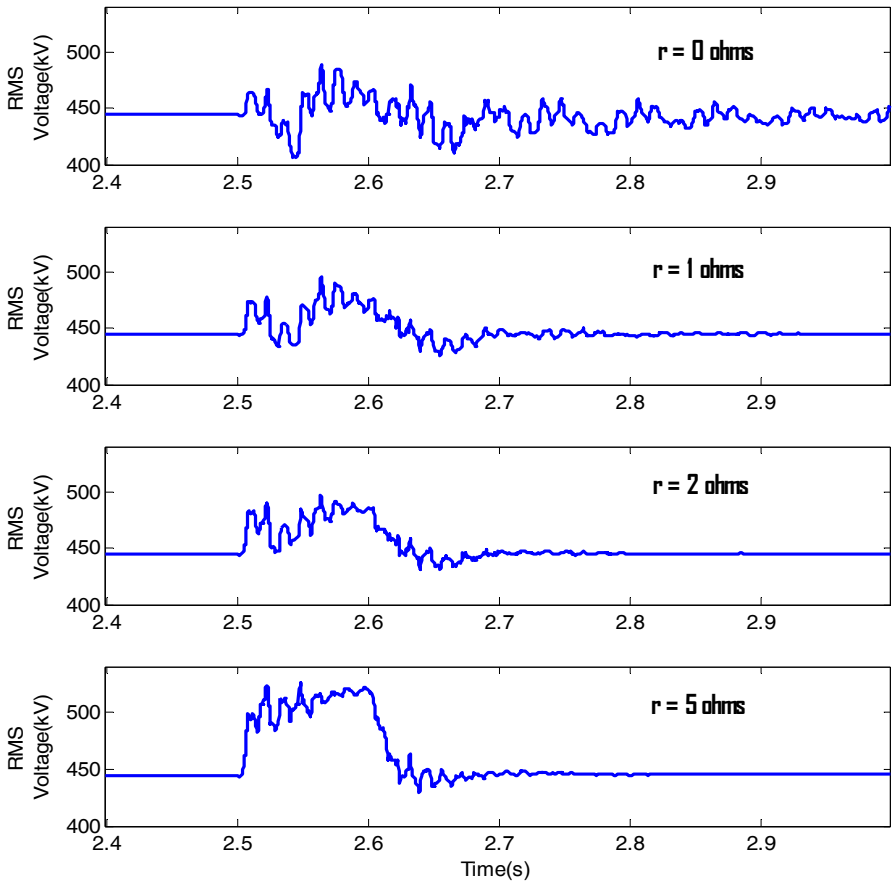

Figure 35: Variations of phase C voltage (rms) on bus-5 during a phase A to ground faultsimulated at bus-3 with different series resistances

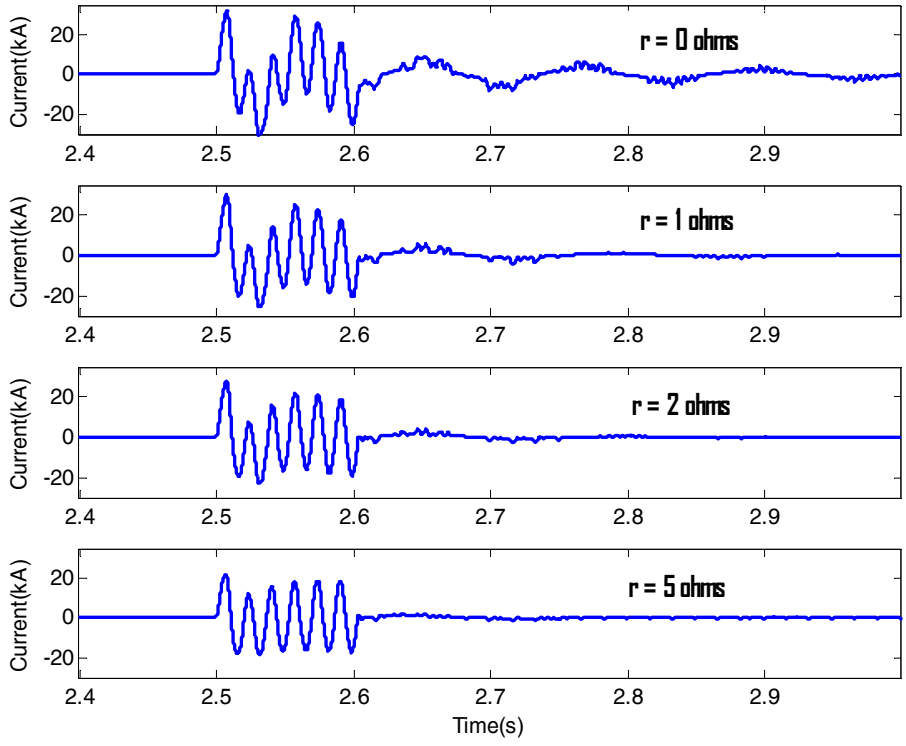

Figure 36: Variations of the neutral current of autotransformer-1 with different series resistances during a phase A to ground fault at bus-3

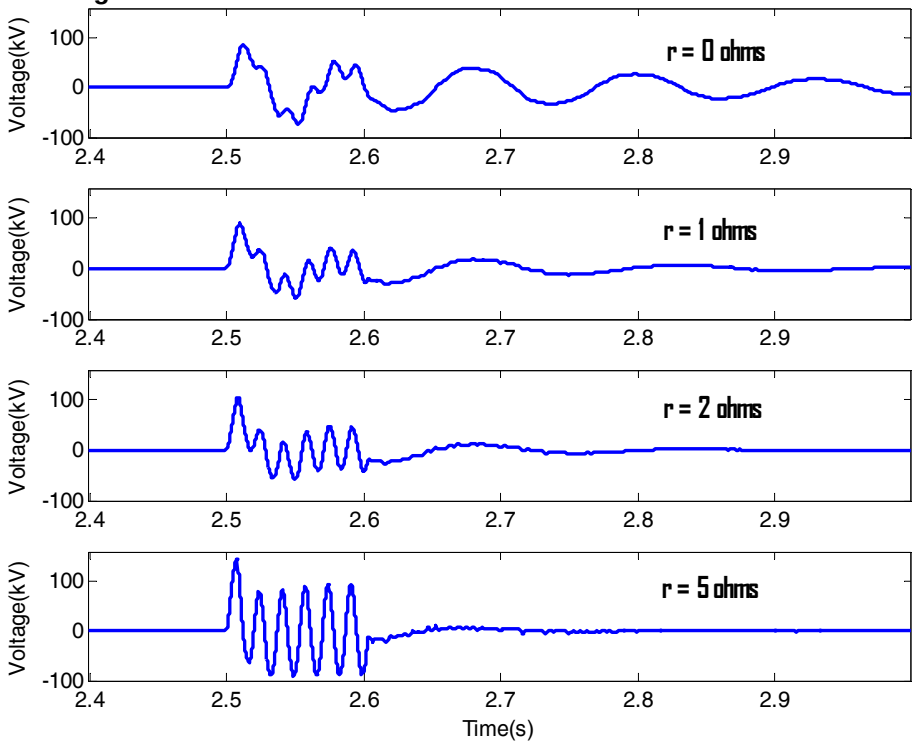

Figure 37: Variation of the neutral voltage of auto transformer-1 with different series resistances during a phase A to ground fault at bus-3

Effect of surge arrester

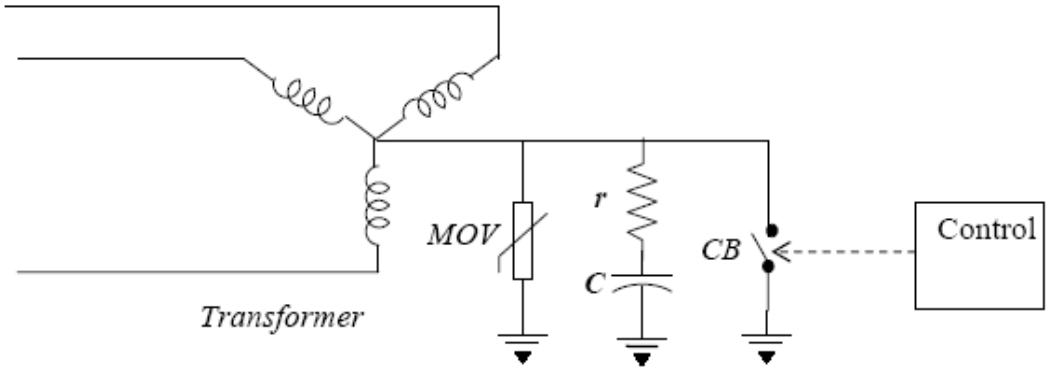

Figure 38: GIC blocking design with a MOV in parallel with the grounding capacitor and resistor

In order to investigate the effect of MOV in reducing excessive neutral voltages and ferroresonance conditions, simulations were carried out. The circuit configuration for these simulations is shown in Figure 38. The value of series resistance was set to 1 ohm. Figure 30 shows the variations of the neutral voltage at autotransformer-2 during a phase A to ground fault simulated at bus-2. The two curves correspond to the cases of with and without MOV. As it can be seen from Figure 39 the use of MOV eliminates the excessive voltages observed at the

transformer neutral during the ground faults. The rating of the MOV used in this simulation was 5 kV.

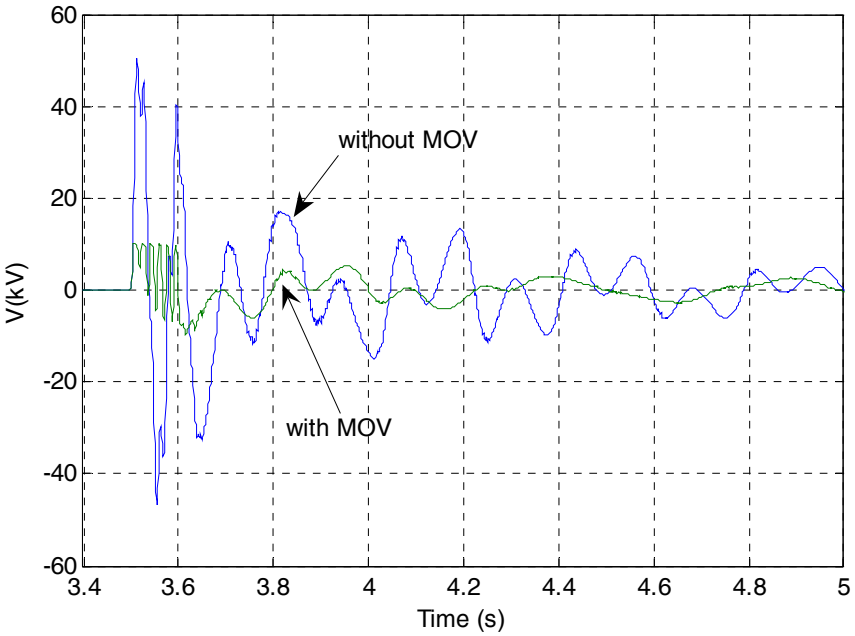

Figure 39: Variation of autotransformer-2 neutral voltage during a phase-A to ground fault at bus 2

Figure 4031 compares the variations of phase C voltage on bus-5 during this fault for the cases of with and without MOV. It can be seen from Figure 40, the operation of the MOV during the high ground currents reduces the oscillations and overvoltages during the fault.

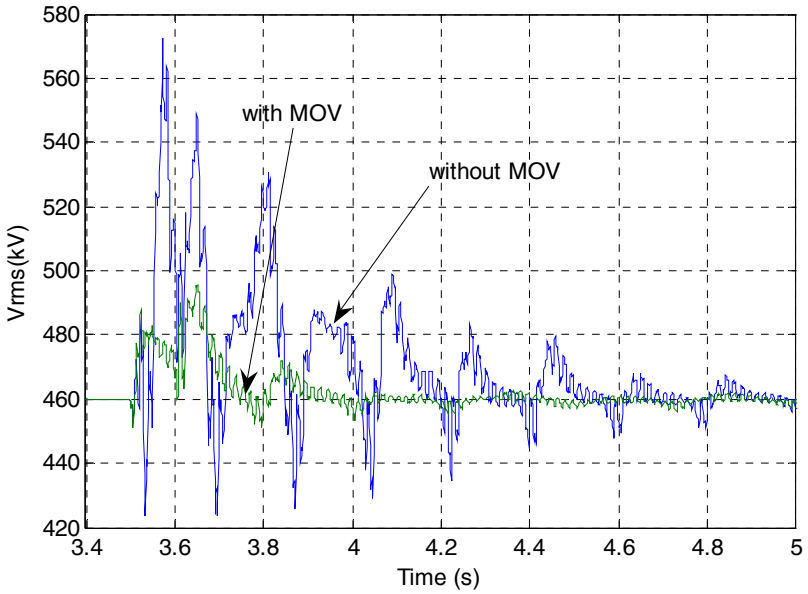

Figure 40: Variation of phase-C rms voltage on bus-5 during a phase-A to ground fault at bus 2

The variations of the current through the MOV and the energy dissipated in it during the fault are shown in Figure 4132.

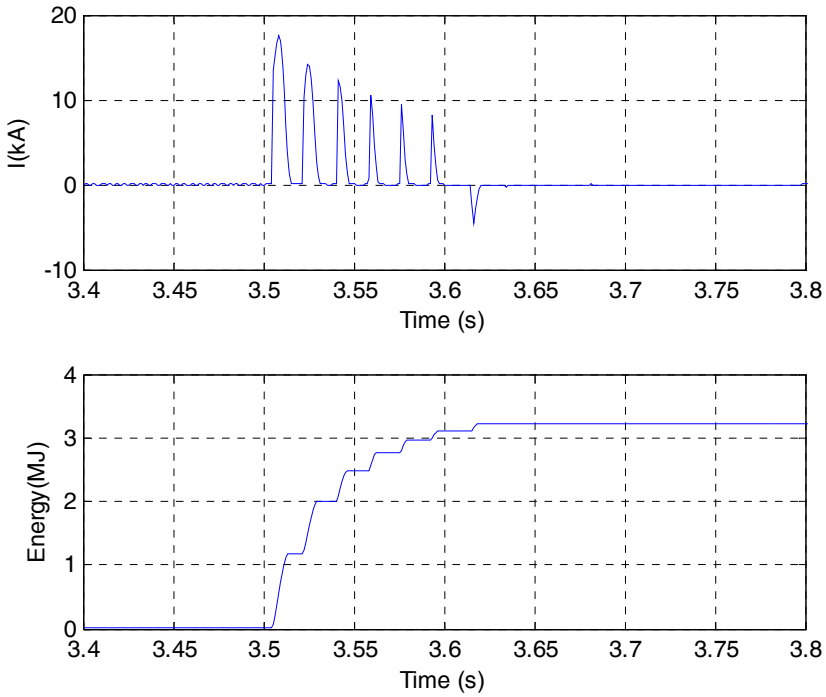

Figure 41: Variations of the current and the energy dissipation in the MOV

Investigation of Possible Conflicts with Existing Transformer Protection Simulations were carried out to investigate the effect of neutral grounding capacitor on the fault levels and the operation of conventional differential protection. The results of this study are summarized below.

Effects on fault levels

Simulations were carried out to investigate the effect of capacitance on the change of fault levels. Ground faults were simulated at different locations of network with and without grounding capacitor. Figures 42 and 43 show the variations of phase current and its rms value with and without the grounding capacitor. The variation of phase current and its rms value with the effect of MOV is also shown in Figure 44. A small reduction in rms value of the fault current was observed due to the insertion of grounding capacitor. With MOV, however, this reduction was not noticeable. The changes to the fault currents due to the grounding capacitor can be essentially neglected.

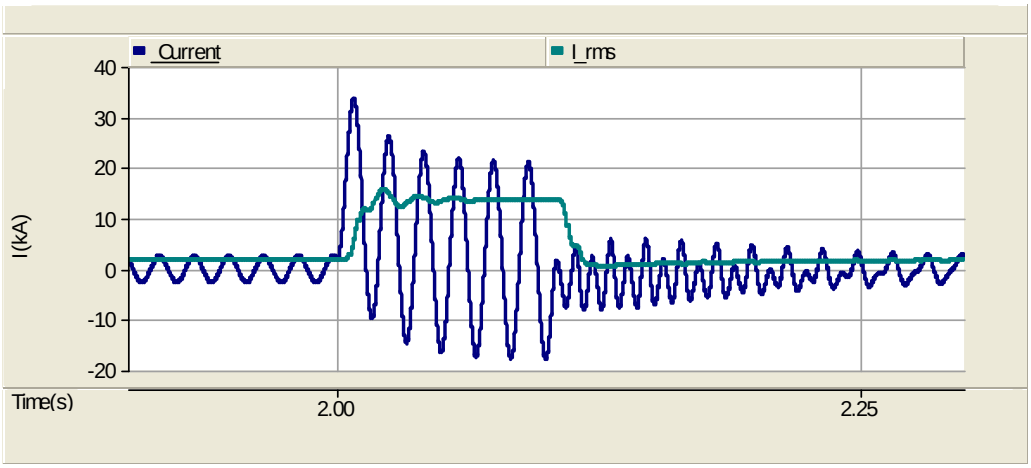

Figure 42: Phase-A winding current and its rms value during a phase A-G fault in the transformer zone - without the grounding capacitor

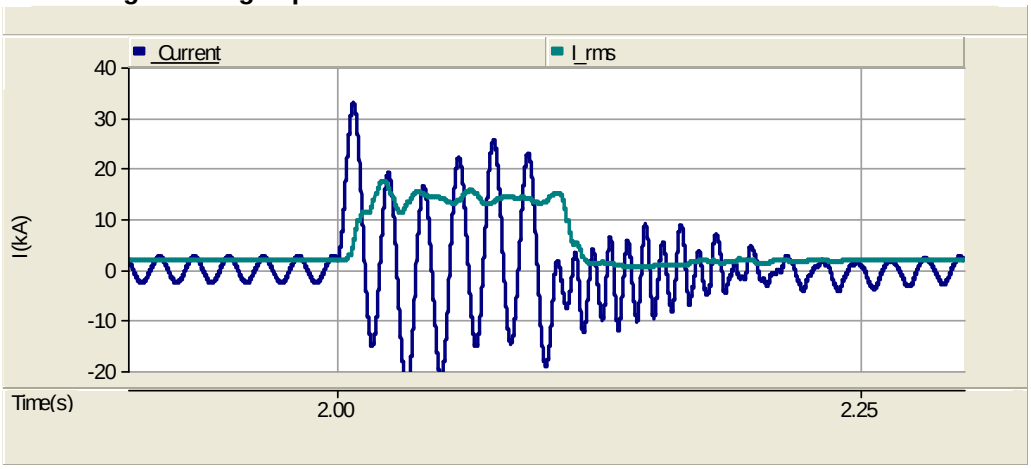

Figure 43: Phase-A winding current and its rms value during a phase A-G fault in the transformer zone - with the grounding capacitor

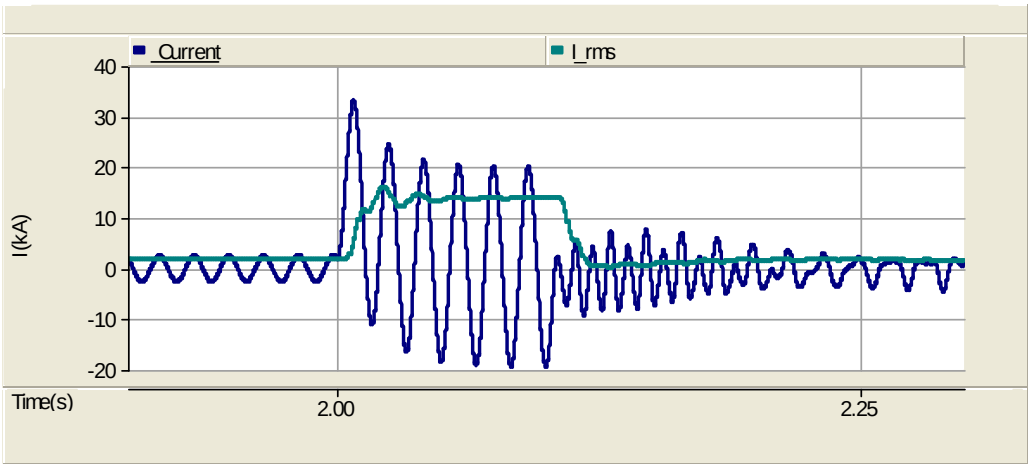

Figure 44: Variation Phase-A winding current and its rms value during a phase A-G fault in the transformer zone - with the grounding capacitor and MOV

Effects on conventional differential protection

In theory, inclusion of a grounding capacitor should not have any effect on the operation of the differential protection. In order to confirm this, simulations based investigation was carried out. A protection design that roughly represents a conventional percentage bias differential protection relay with a single slope characteristic was simulated for auto-transformer-1. Different types of internal and external faults were simulated at different locations of the network with and without the effect of the grounding capacitor. As expected, the differential protection operated normally even when the capacitor was present. Some sample simulation results are shown below.

Figures 45 and 46 shows the operation of conventional differential protection on auto-transformer-1 during a phase-to-phase (A-B) internal fault for the cases of without and with the grounding capacitor respectively. The third graph from the top of both Figures 45 and 46 show the variations of the differential (operating) (Fdiff) and restraining (Fres) current components. The differential protection operates when the differential current exceeds a certain percentage (determined by the slope characteristics) of the restraining current.

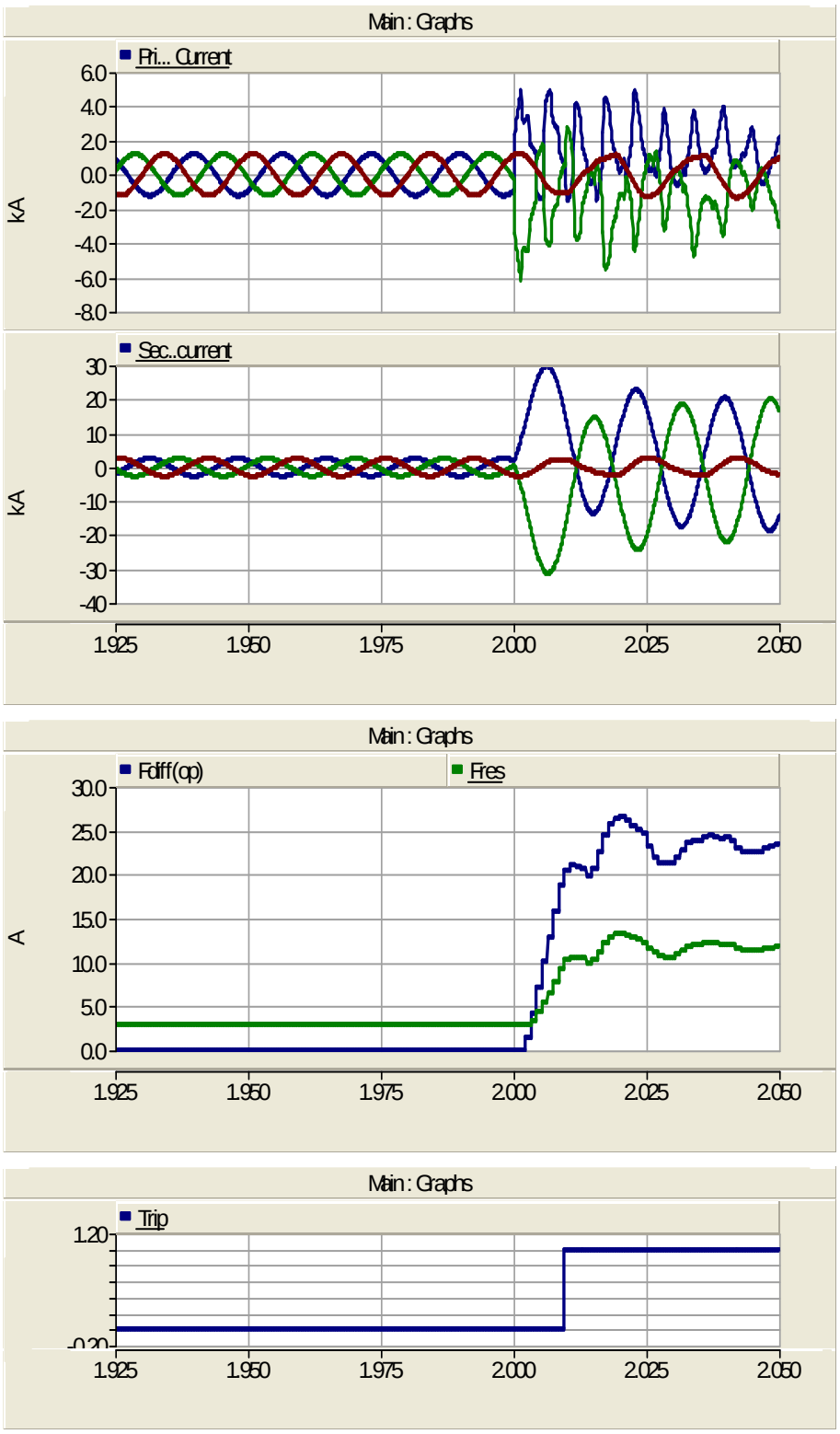

Figure 45: Variations of the Autotransformer-1 primary/secondary currents, phase-A restraining/operating currents and the trip signal during a Phase A-B internal fault - without the grounding capacitor.

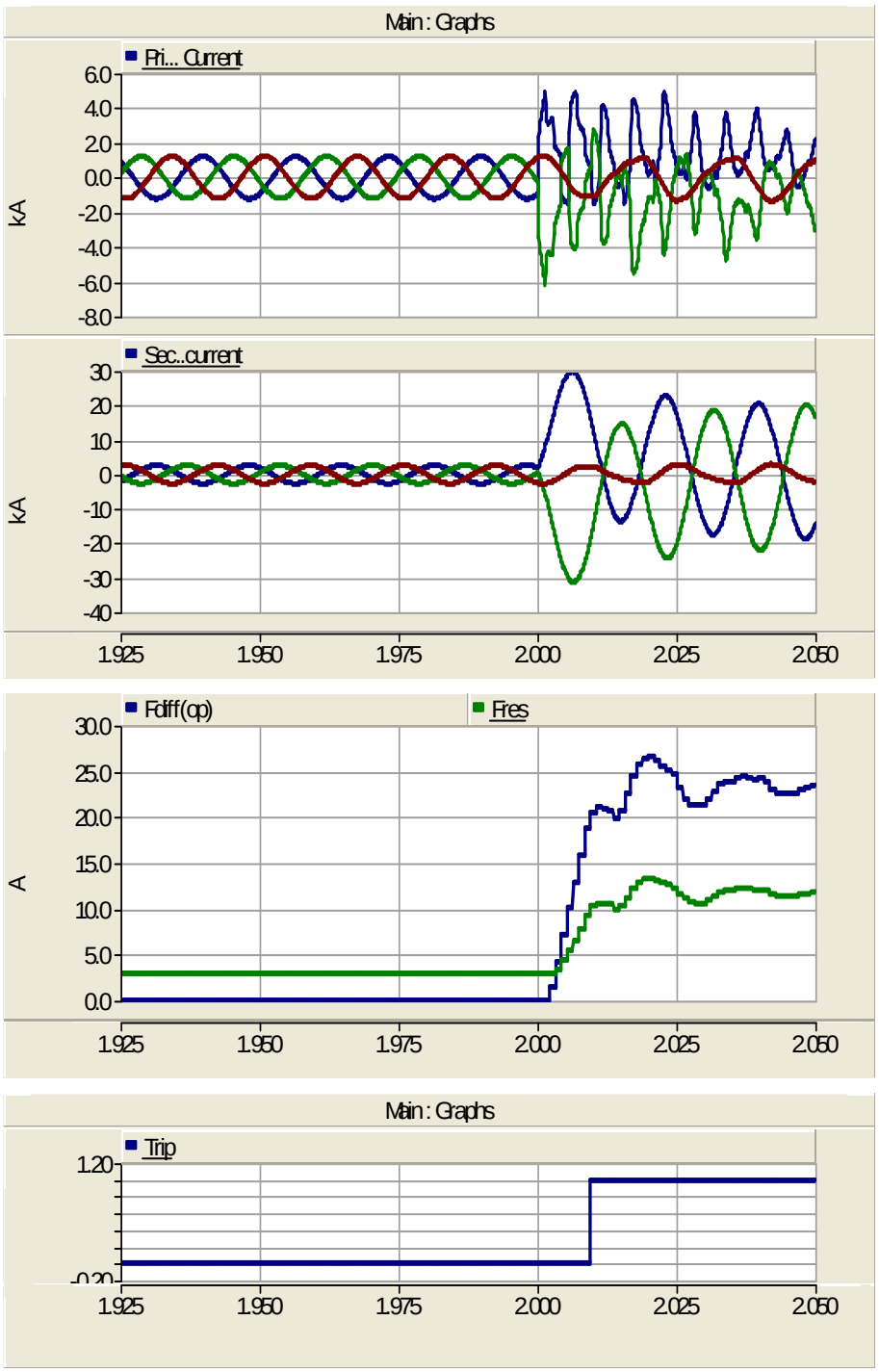

Figure 46: Variations of the Autotransformer-1 primary/secondary currents, phase-A restrain/operating currents and the trip signal during a Phase A-B internal fault - with the grounding capacitor

Figures 47 and 48 shows the operation of conventional differential protection on autotransformer-1 during a phase-to-ground (A-G) internal fault for the cases of without and with the grounding capacitor respectively.

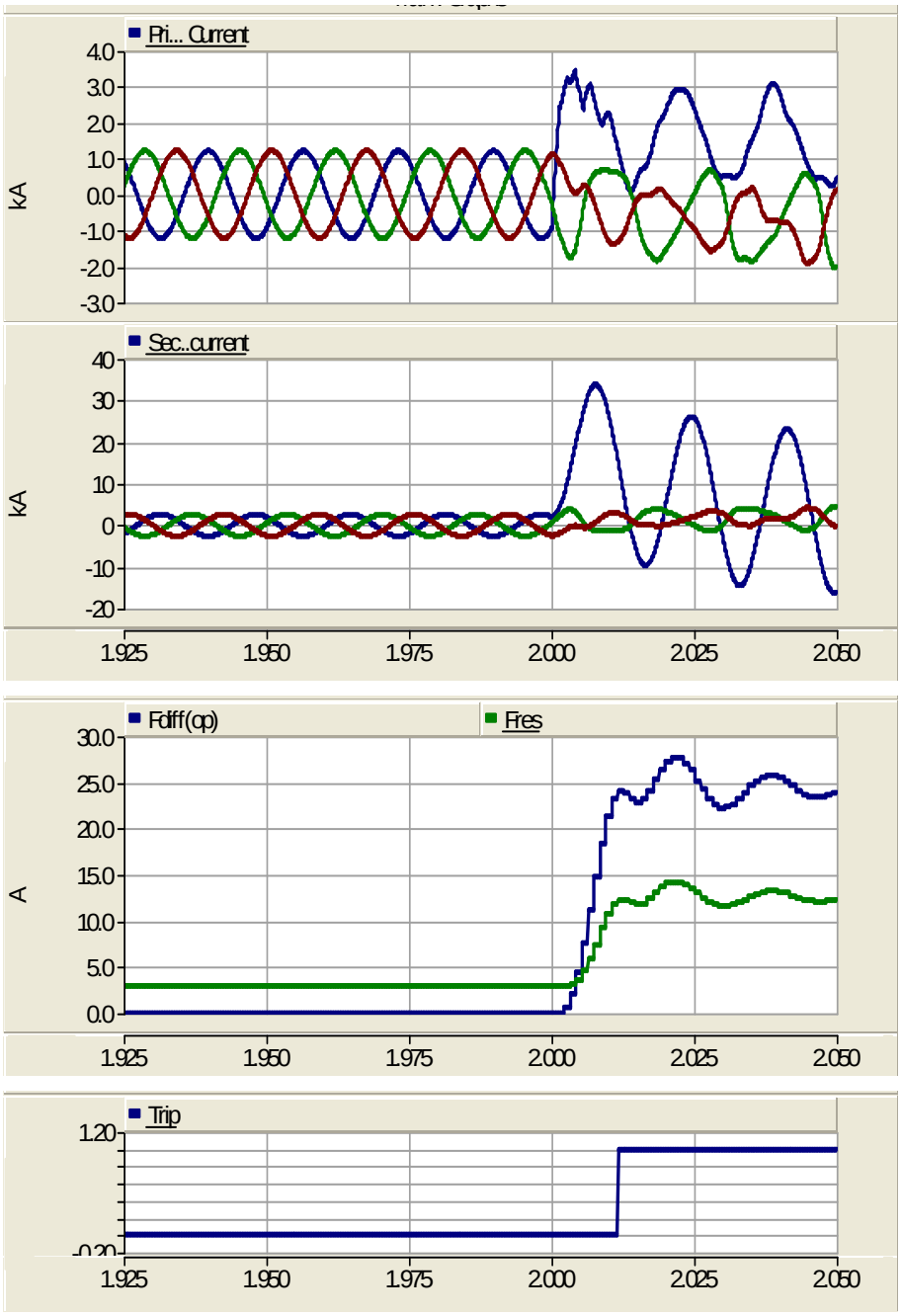

Figure 47: Variations of the transformer primary/secondary currents, phase-A restrain/operating currents and the trip signal during a phase A-G internal fault - without the grounding capacitor

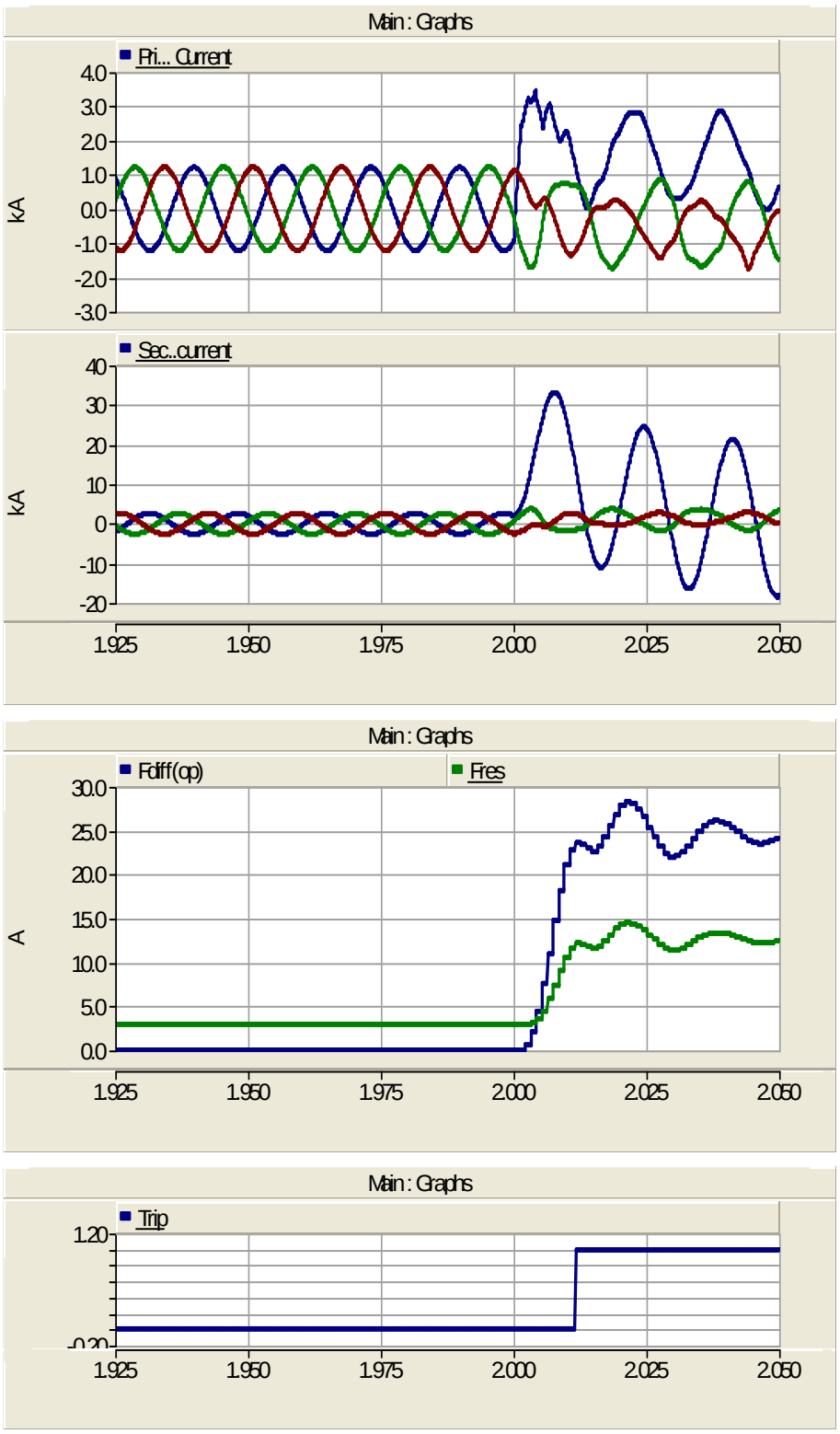

Figure 48: Variations of the transformer primary/secondary currents, phase-A restrain/operating currents and the trip signal during a phase A-G internal fault - with the grounding capacitor

The behavior of the differential protection during a single phase to ground fault external to the transformer (on bus-3) is shown in Figure 49 and 50 for the cases of without and with the grounding capacitor respectively.

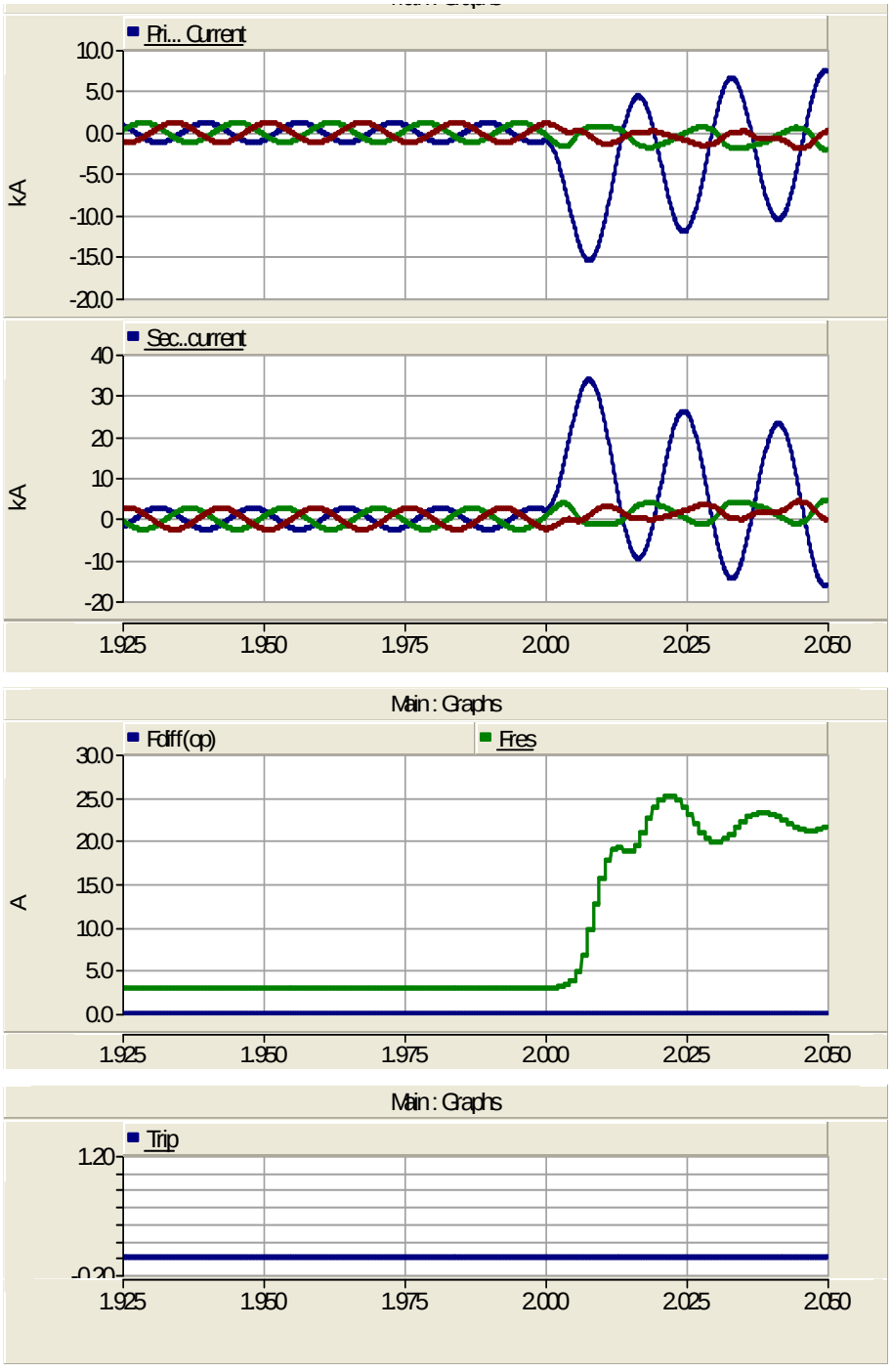

Figure 49: Variations of the transformer primary/secondary currents, phase-A restrain/operating currents and the trip signal during Phase A-G external fault - without the grounding capacitor

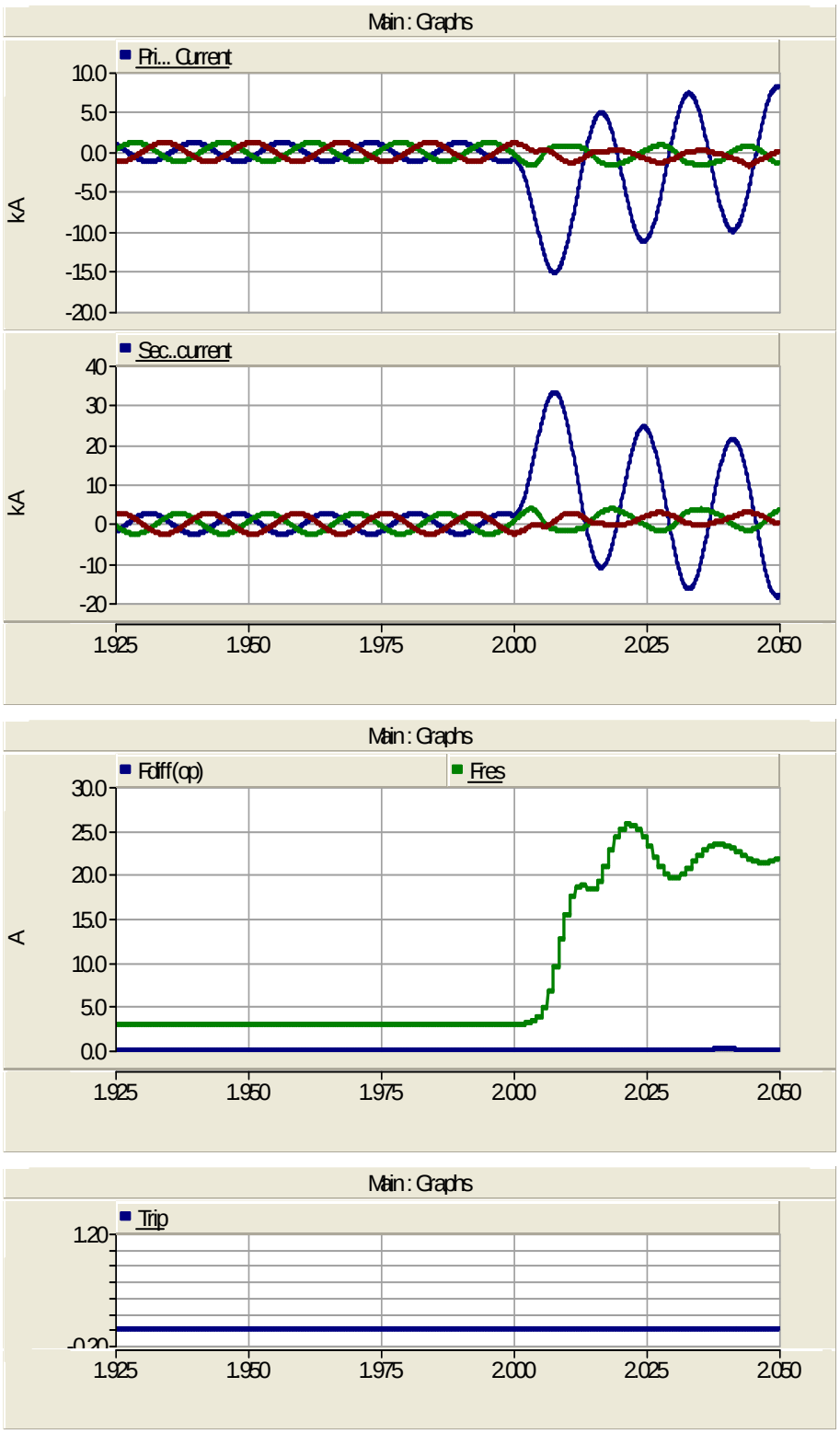

Figure 50: Variations of the transformer primary/secondary currents, phase-A restrain/operating currents and the trip signal during a Phase A-G external fault - with the grounding capacitor

Effects on restricted earth fault protection

The restricted earth fault (REF) protection is one of the common types of protection used for transformers protection. This protection also operates based on the principle of differential currents. Simulations were also carried out to investigate the effect of the grounding capacitor on the operation of REF protection of Autotransformer-1. Figures 51 and 52 show the operation of REF protection during an internal Phase-A to ground fault for the cases of with and without the grounding capacitor.

The top two graphs in Figure 51 (and 52-54) show the variations of the phase currents at the primary and the secondary sides. The third graph from the top shows the variations of the residual current (Ia+Ib+Ic) of primary/secondary windings and the transformer neutral current. The fourth graph from the top shows the variations of the operating and restraining signals. The bottom graph shows the trip signal.

Operation of the REF protection during external ground faults was also investigated. Figures 53 and 54 show the behavior of REF protection during an external Phase-A to ground fault for the cases of without and with the grounding capacitor.

Results obtained in this study showed that the operation of conventional differential protection and restricted earth fault protection was not affected by the grounding capacitor.

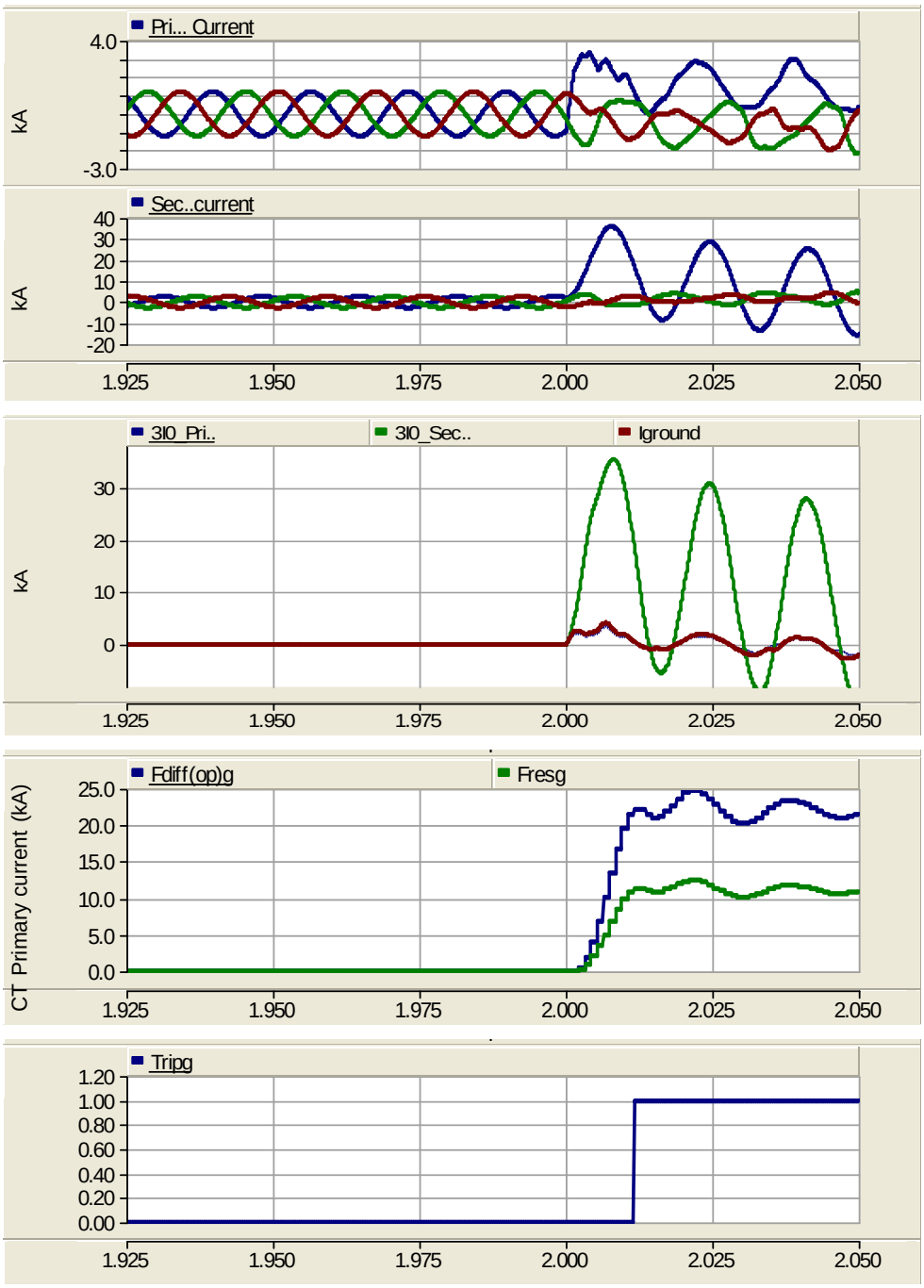

Figure 51: Variations of the Autotransformer-1 primary/secondary phase currents, primary and secondary residual currents, corresponding restrain/operating currents and the trip signal during a Phase A-G internal fault - without the grounding capacitor

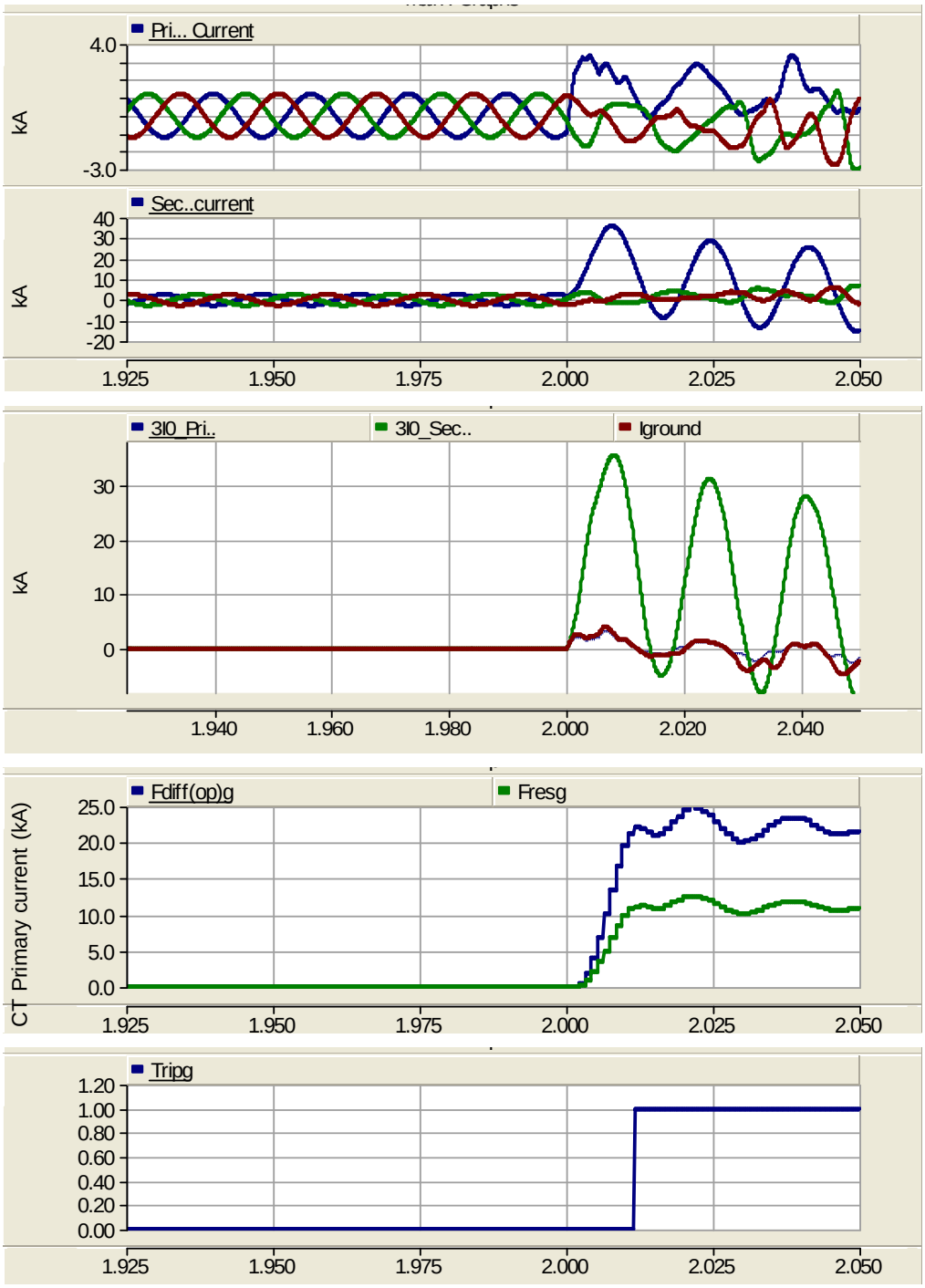

Figure 52: Variations of the Autotransformer-1 primary/secondary phase currents, primary and secondary residual currents, corresponding restrain/operating currents and the trip signal during a Phase A-G internal fault - with the grounding capacitor

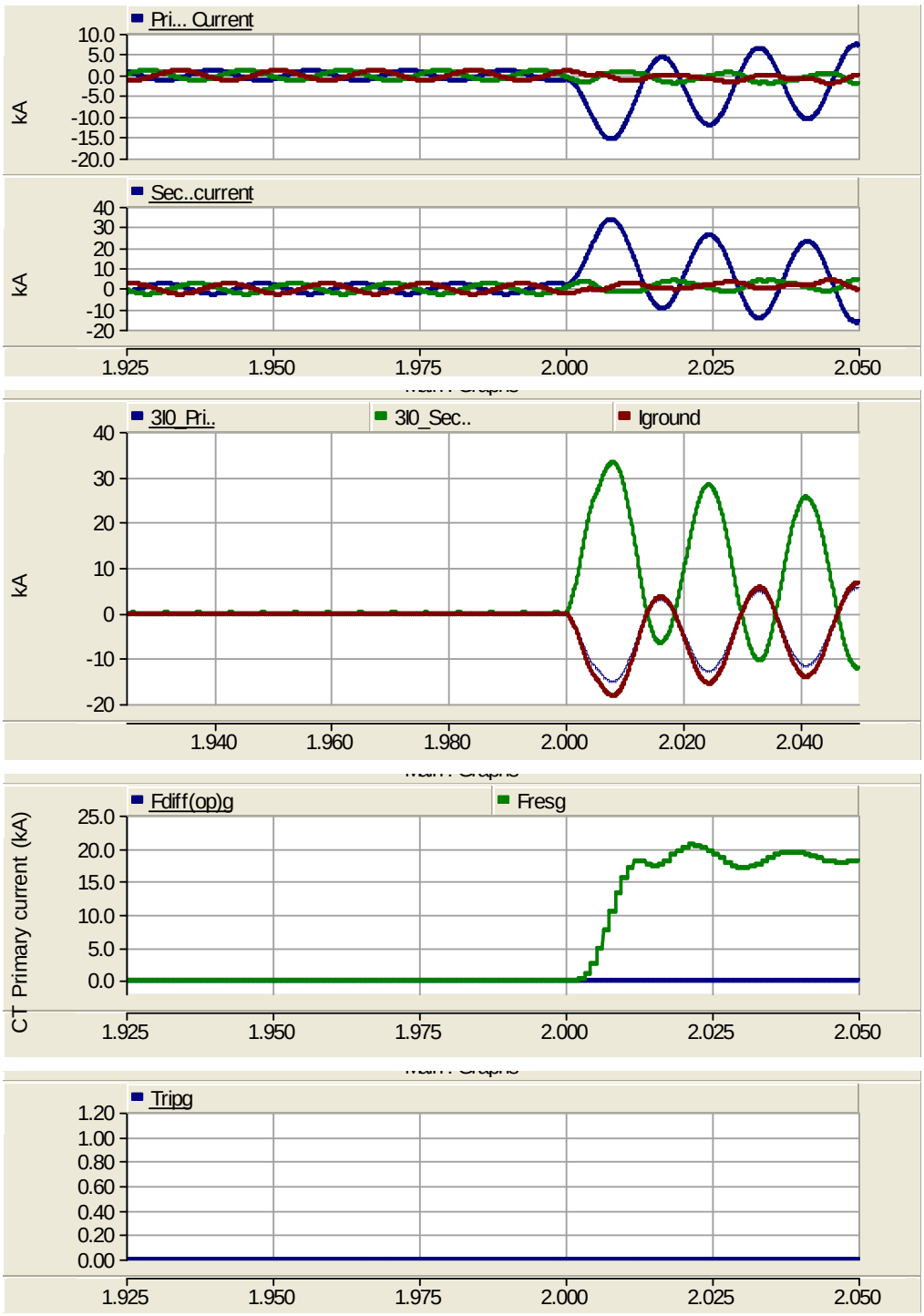

Figure 53: Variations of the Autotransformer-1 primary/secondary phase currents, primary and secondary residual currents, corresponding restrain/operating currents and the trip signal during a Phase A-G external fault - without the grounding capacitor

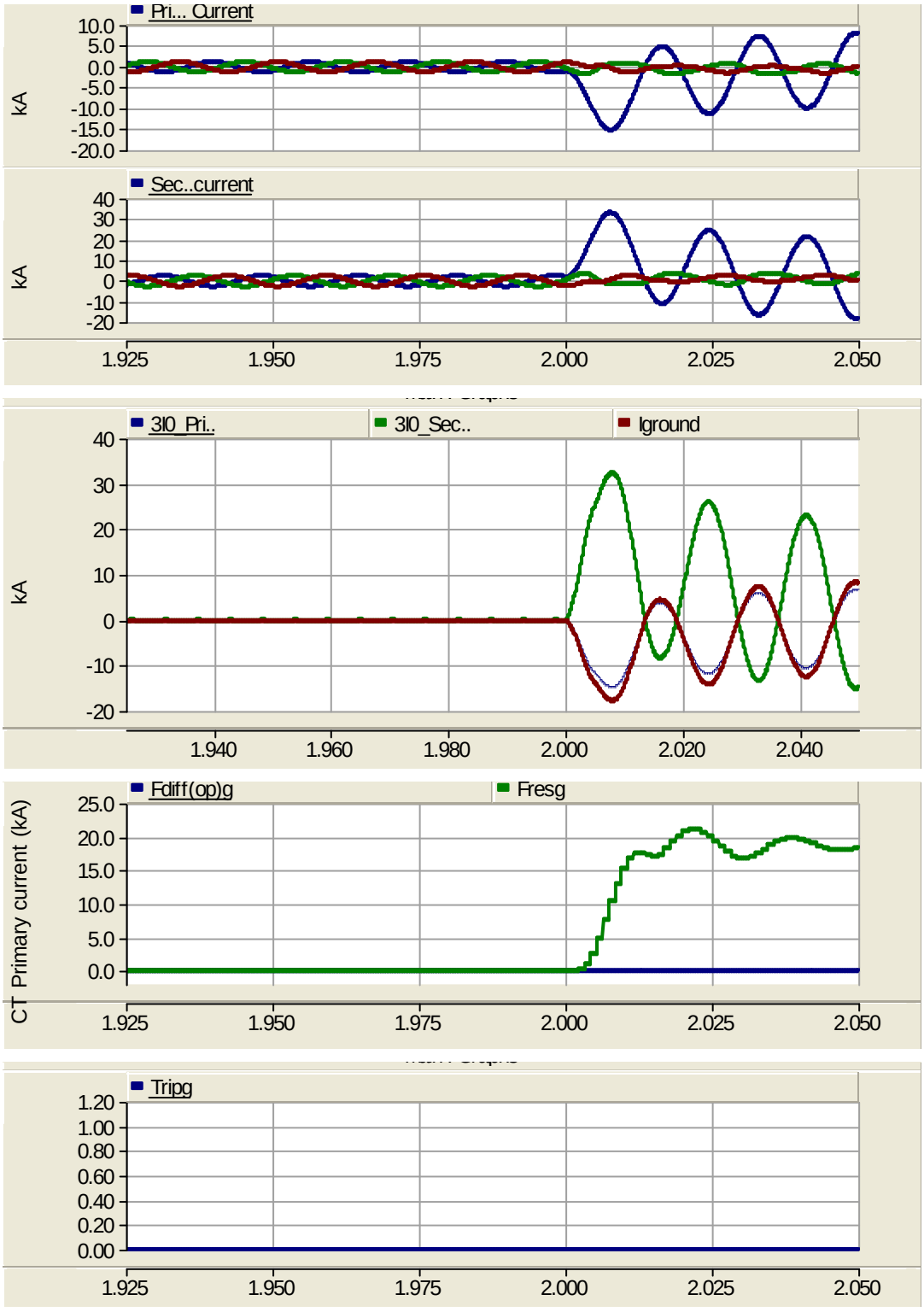

Figure 54: Variations of the Autotransformer-1 primary/secondary phase currents, primary and secondary residual currents, corresponding restrain/operating currents and the trip signal during a Phase A-G external fault - with the grounding capacitor

6. Conclusions

The studies were carried out to investigate the validity of the proposed GIC mitigation concept.

Simulations were carried out using a transmission system simulated in electromagnetic (EMT) type simulation program PSCAD/EMTDC.

Results showed the potential in reducing quasi-DC current that causes the saturation of transformers during GIC events using the proposed GIC mitigation concept.

Simulations also showed an evidence of high neutral voltages and ferroresonance conditions during ground faults when the proposed mitigation is active.

Applicability of different methods to reduce effects of high neutral currents and ferroresonance conditions was investigated. The results show that, adding a resistance in series with the capacitor helps to reduce the oscillations observed in the neutral voltage after a ground fault was introduced. Results also showed that the use of surge arrester in parallel with the capacitor and resistor significantly reduces the ferroresonance oscillations and overvoltages after a ground fault was introduced.

The effect of the proposed mitigation on the performance of the conventional protection schemes of transformers was also investigated. The results showed that the operation of conventional protection was not impacted by the grounding capacitor.

A manuscript titled “Transformer Protection against GIC Using a Capacitive Grounding Circuit” was prepared summarizing the results.

7. References

[1] F.S. Prabhakara, L.N. Hannett, R.I Ringlee, J.Z. Ponder, "Geomagnetic effects modelling for the PJM interconnection system. II. Geomagnetically induced current study results" *IEEE Trans. on Power Systems*, vol.7, no.2, pp.565-571, May 1992.

[2] V.D. Albertson, B. Bozoki, W.E. Feero, J.G. Kappenman, E.V. Larsen, D.E. Nordell, J. Ponder, F.S. Prabhakara, K. Thompson, and R. Walling, “Geomagnetic disturbance effects on power systems," *IEEE Trans. on Power Delivery*, vol.8, no.3, pp.1206-1216, July 1993.

[3] J.G. Kappenman, V.D. Albertson, N. Mohan, "Current Transformer and Relay Performance in the Presence of Geomagnetically Induced Currents," *IEEE Trans. on Power Apparatus and Systems*, vol-100, no.3, pp.1078-1088, March 1981.

[4] M.A.S. Masoum, P.S. Moses, “Influence of Geomagnetically Induced Currents on three-phase power transformers" *Australasian Universities Power Engineering Conference, 2008*, pp.1-5, Dec. 2008.

[5] W. Chandrasena, “Development of an improved low frequency transformer model for use in GIC studies”, Thesis (Ph.D.) Dissertation, Dept. of Electrical and Computer Engineering, University of Manitoba, 2004.

[6] L. Bolduc, P. Langlois, D. Boteler, and R. Pirjola, "A study of geoelectromagnetic disturbances in Quebec. II. Detailed analysis of a large event," *IEEE Trans. on Power Delivery*, vol. 15, pp. 272-278, 2000.

[7] J.G. Kappenman, S.R. Norr, G.A. Sweezy, D.L. Carlson, V.D. Albertson, J.E. Harder, B.L. Damsky, "GIC mitigation: a neutral blocking/bypass device to prevent the flow of GIC in power systems," *IEEE Trans. on Power Delivery*, vol.6, no.3, pp.1271-1281, Jul 1991.

[8] M. A. Eitzmann, R. A. Walling, M. Sublich, A. Khan, H. Huynh, M. Granger, and A. Dutil, “Alternatives for blocking direct current in AC system neutrals at the Radisson/LG2 complex,” IEEE Trans. Power Delivery, vol. 7, pp. 1328–1337, July 1992.

[9] J. G. Kappenman and S. R. Norr, “Neutral blocking device combats currents caused by geomagnetic storms—Designed to reduce power system vulnerability during high sunspot activity,” Transm. Distrib., vol. 44, no. 5, pp. 46–54, May 1992.

[10] L. Bolduc, M. Granger, G. Pare, J. Saintonge, L.Brophy, "Development of a DC current-blocking device for transformer neutrals," *IEEE Trans. on Power Delivery,* vol.20, no.1, pp. 163- 168, Jan. 2005.

[11] “GIC blocking device and DEI application note #5: Blocking DC current in transformer neutrals,” DEI Dairyland Electrical Industries, Stoughton, WI.

[12] USER’S GUIDE 2005, A Comprehensive Resource for EMTDC: Transient Analysis for PSCAD Power System Simulation, *Manitoba HVDC Research Centre Inc.*, Winnipeg, Manitoba, Canada.

[13] R.J. Edwards, Typical Soil Characteristics of Various Terrains, 1998, Available at http://www.smeter.net/grounds/soil-electrical-resistance.php

[14] Dimensioning, testing and applications of metal oxide surge arrester in low voltage power distribution systems, Application Guide: Over Voltage Protection, *ABB High Voltage Technologies Lt*d, Wettingen, Apr. 2001.

8. Appendix

Transmission line parameters

TABLE-I- LINE PARAMETERS

Line	Type	Length	+/0 Seq. Impedance (Ω)
Bus 2-3	Double circuit	400 km	4.97+135.44j/ 115.35+435.14j
Bus 3-5	Single circuit	200 km	2.48 +67.72j/ 57.68+217.57j

Transformer parameters

TABLE-II- TRANSFORMER PARAMETERS

Transformer	Capacity	Leakage reactance	No load losses	Copper losses at rated current
Auto-transformer-1	900 MVA 765 kV/345kV	0.01 pu	0.015 pu	0.02 pu
Auto-transformer-2	300 MVA 765 kV/22kV	0.01 pu	0.015 pu	0.02 pu
Std. transformer	1000 MVA DY-22kV/65kV	0.01 pu	0.015pu	0.02 pu

MOV characteristics

TABLE-III- MOV CHARACTERISTICS

Current (kA)	Voltage (kV)	Current (kA)	Voltage (kV)
0.0001	5.0	0.6	9.265
0.02	5.5	0.8	9.405
0.1	7.0	1.0	9.5
0.25	8.695	2.0	15.0
0.4	9.075	100.0	16.0